

APPENDICES

APPENDIX A: BRIDGE DRAWINGS AND PHOTOS

APPENDIX A: BRIDGE DRAWINGS AND PHOTOS

List of Figures

Figure A-1: Bridge location.....	2
Figure A-2: Horsetail Creek Bridge	2
Figure A-3: Bridge during retrofit	3
Figure A-4: Typical formwork w/ steel	3
Figure A-5: Strain gauge application	3
Figure A-6: Replicated steel reinforcing	3
Figure A-7: Typical beam pour	4
Figure A-8: Surface preparation: abrasion	4
Figure A-9: Fiber optic gauge placement.....	4
Figure A-10: Tack coat and epoxy application.....	4
Figure A-11: Saturation of CFRP w/ epoxy.....	4
Figure A-12: Epoxy application.....	4
Figure A-13: GFRP application to test beams.....	5
Figure A-14: CFRP application to test beam.....	5
Figure A-15: In situ epoxy mixing	5
Figure A-16: CFRP application to test beam.....	5
Figure A-17: Second coat of epoxy/CFRP.....	5
Figure A-18: Completed carbon reinforcement	5
Figure A-19: Testing of Control beam	6
Figure A-20: Early cracking of Control beam.....	6
Figure A-21: Control beam shear sections.....	6
Figure A-22: Shear failure of Control beam.....	6
Figure A-23: Shear failure through sections.....	6
Figure A-24: Completed shear failure.....	6
Figure A-25: Crack pattern around failure.....	7
Figure A-26: Support point: rotation at failure	7
Figure A-27: Load point: crushing at failure	7
Figure A-28: Flexure-only beam testing.....	7
Figure A-29: Failure of Flexure-only beam	7
Figure A-30: Diagonal tension failure	7
Figure A-31: Failure similar to Control beam.....	8
Figure A-32: CFRP transverse rupture	8
Figure A-33: Fiber optic.....	8
Figure A-34: Cracking at failure	8
Figure A-35: Flexure-only beam at failure	8
Figure A-36: Load point at failure	9
Figure A-37: Debonding of CFRP at support.....	9
Figure A-38: Fiber optic comparison gauges.....	9
Figure A-39: Overall view of Shear-only test	9
Figure A-40: Loading of Shear-only beam	10
Figure A-41: Failure of Shear-only	10
Figure A-42: Concrete crushing at midspan.....	10
Figure A-43: Shear-only beam support point.....	10
Figure A-44: S&F deflection under high load	10
Figure A-45: Visible S&F beam deflections.....	11
Figure A-46: S&F beam shear sections.....	11
Figure A-47: Maximum loading of S&F beam.....	11
Figure A-48: Increase moment max. loading.....	11

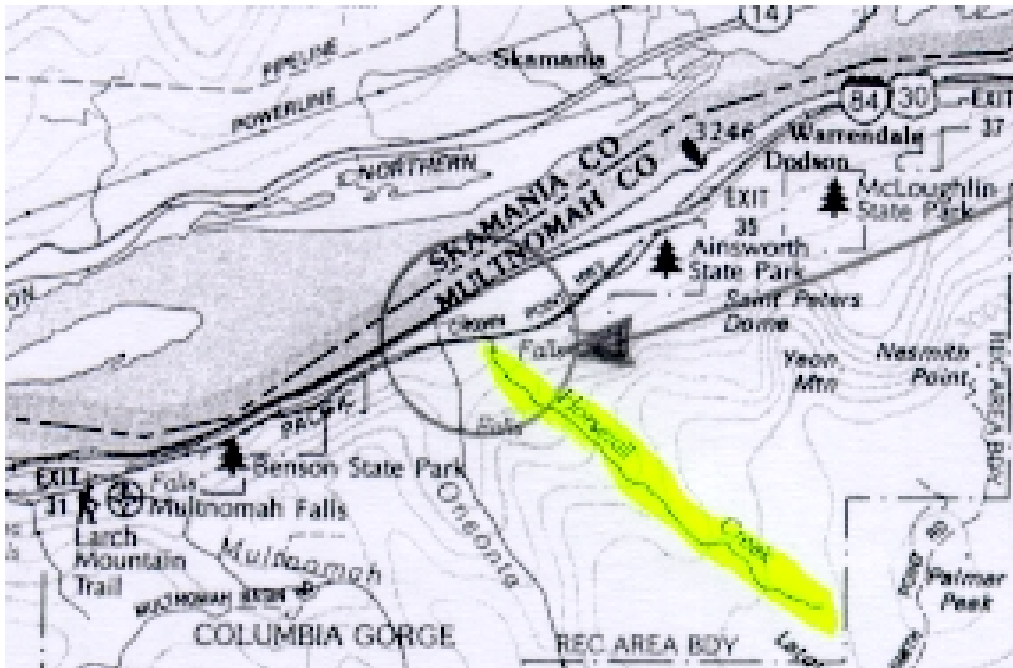


Figure A-1: Bridge location



Figure A-2: Horsetail Creek Bridge



Figure A-3: Bridge during retrofit



Figure A-4: Typical formwork w/ steel



Figure A-5: Strain gauge application



Figure A-6: Replicated steel reinforcing



Figure A-7: Typical beam pour



Figure A-8: Surface preparation: abrasion



Figure A-9: Fiber optic gauge placement



Figure A-10: Tack coat and epoxy application



Figure A-11: Saturation of CFRP w/ epoxy



Figure A-12: Epoxy application



Figure A-13: GFRP application to test beams



Figure A-16: CFRP application to test beam



Figure A-14: CFRP application to test beam



Figure A-17: Second coat of epoxy/CFRP



Figure A-15: In situ epoxy mixing



Figure A-18: Completed carbon reinforcement



Figure A-19: Testing of Control beam



Figure A-22: Shear failure of Control beam



Figure A-20: Early cracking of Control beam



Figure A-23: Shear failure through sections



Figure A-21: Control beam shear sections



Figure A-24: Completed shear failure

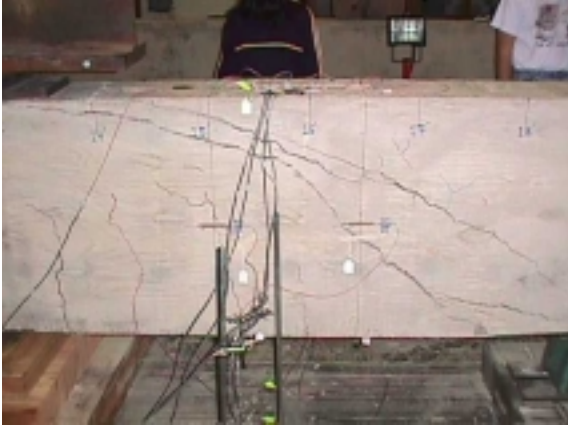


Figure A-25: Crack pattern around failure



Figure A-28: Flexure-only beam testing



Figure A-26: Support point: rotation at failure



Figure A-29: Failure of Flexure-only beam



Figure A-27: Load point: crushing at failure



Figure A-30: Diagonal tension failure



Figure A-31: Failure similar to Control beam



Figure A-34: Cracking at failure



Figure A-32: CFRP transverse rupture



Figure A-35: Flexure-only beam at failure



Figure A-33: Fiber optic

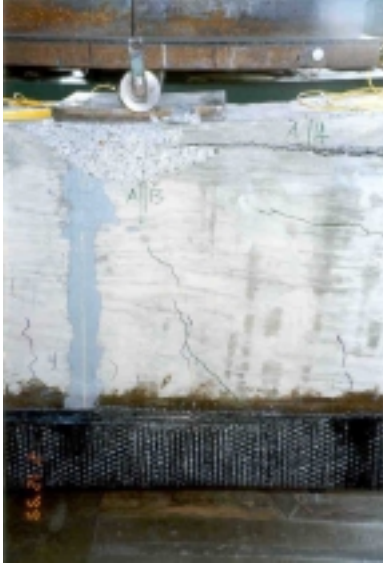


Figure A-36: Load point at failure



Figure A-38: Fiber optic comparison gauges



Figure A-37: Debonding of CFRP at support



Figure A-39: Overall view of Shear-only test



Figure A-40: Loading of Shear-only beam



Figure A-41: Failure of Shear-only



Figure A-42: Concrete crushing at midspan



Figure A-43: Shear-only beam support point

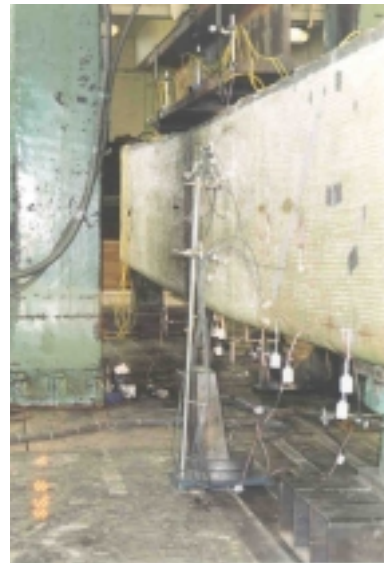


Figure A-44: S&F deflection under high load



Figure A-45: Visible S&F beam deflections



Figure A-47: Maximum loading of S&F beam



Figure A-46: S&F beam shear sections



Figure A-48: Increase moment max. loading

**APPENDIX B: CALCULATIONS FOR LOAD RATING AND
DESIGN OF EXPERIMENTAL BEAMS**

APPENDIX B: CALCULATIONS FOR LOAD RATING AND DESIGN OF EXPERIMENTAL BEAMS

Load Rating Calculations

For any structural element resisting forces on a bridge the Rating Factor (RF) is defined as

$$RF = \frac{\phi R_n - \gamma_{DL}(DL)}{(DF)\gamma_{DL}(LL)(1+I)} \quad [B-1]$$

This equation originates from the American Association of State and Highway Transportation Officials, Manual for Condition Evaluation of Bridges (AASHTO, 1994) and Guide Specifications for Strength Evaluation of Existing Steel and Concrete Bridges (AASHTO, 1989). These specifications establish the way in which state and local agency bridges are evaluated. For reinforced concrete beams, Load and Resistance Factor Design (LRFD) is used, as is apparent in equation [B-1]. A description of variables is given in Table B-1. According to this method, if the RF for a specific element is less than 1.0, then the capacity of that element is considered inadequate for the conditions.

CH2M HILL in conjunction with TAMS Consultants (CH2M HILL, 1997) performed a load rating for Horsetail Falls Bridge. The analysis is shown below.

Table B-1: Load Equation Rating Variables

Variable	Description	Horsetail Shear Load Rating Value	Horsetail Moment Load Rating Value
R_n	Nominal capacity of the structural member (e.g. shear or moment capacity)	$V_n = 31.2$ kip ($V_n = 37.2$ kip) [†]	$M_n = 341$ ft-kip
ϕ	Strength reduction factor.	0.85	0.90
γ_{DL}, γ_{LL}	Dead and live load factors, respectively.	1.20, 1.30	1.20, 1.30
DL, LL	Maximum dead and live load effects as calculated from the analysis.	See calcs.	See calcs.
I	Impact factor to account for uncertainty in dynamic loading.	0.10	0.10
DF	Distribution factor which accounts for wheel distribution per lane. These are essentially influence ordinates.	Single = 0.767, Multiple = 1.033	Single = 3.50, Multiple = 5.00

[†] Nominal shear capacity using the more detailed shear capacity equations. Not used here.

Load Rating of Horsetail for Flexural Capacity

The applied load configuration used in the load rating of HCB crossbeams is shown in Fig. B-1. An HS20 legal load truck was used in the analysis (32-kip axle).

The nominal moment capacity of the HCB crossbeams based on conventional reinforced concrete beam theory with tension reinforcement only is

$$M_n = A_s f_y (d - a/2) \quad [B-2]$$

where

$$a = (A_s f_y) / (0.85 f_c' b) \quad [B-3]$$

This is a close approximation provided the beam is ductile (steel yields before crushing of the concrete). The properties for the crossbeams were assumed according to unknown material properties for bridges built before 1959 and in lieu of testing (AASHTO, 1989, Ch. 6). Using information from the original plans:

$$a = (5.00 \text{ in}^2 * 33,000 \text{ psi}) / (0.85 * 2500 \text{ psi} * 12 \text{ in})$$

$$a = 6.471 \text{ in}$$

$$M_n = (5.00 \text{ in}^2 * 33,000 \text{ psi}) (28.0 \text{ in} - (6.471 \text{ in} / 2))$$

$$M_n = 4,086,200 \text{ lb-in} = 341 \text{ kip-ft}$$

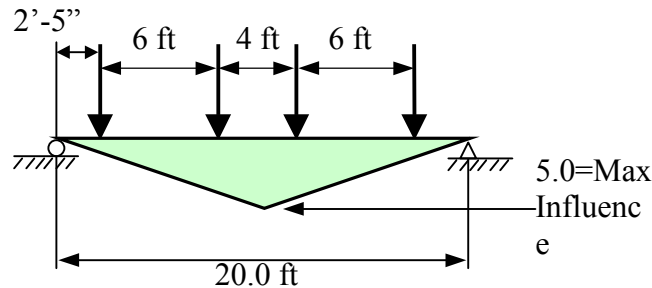


Figure B-1: Truck position to induce maximum positive-moment influence in crossbeams (simply supported)

From Figure B-1, the total positive moment influence from the two trucks positioned on the crossbeam is calculated by the influence ordinates. For this arrangement, the total influence is the sum of 0.7917, 3.792, 4.208, 1.208 and divided by two since there are two lanes. Thus the distribution factor is 5.0. Using the moment capacity, the calculated live and dead loads (CH2M Hill, 1997) and the load rating equation [B-1], the rating factor for positive moment is

$$RF_{\text{flexure}} = \frac{(0.85 * 341 \text{ ft - kip}) - (1.20 * 107 \text{ ft - kip})}{(5.0) * (1.30 * 45.0 \text{ ft - kip}) * (1.10)}$$

or

$$RF_{\text{flexure}} = \frac{(0.9 * 341 \text{ ft - kip}) - (1.20 * 107 \text{ ft - kip})}{(1.033) * (1.10) * (1.30) * (240.66 \text{ ft - kip})}$$

$$RF_{\text{flexure}} = 0.50$$

Load Rating of Horsetail for Shear Capacity

The live load distribution used in the load rating of HCB crossbeams for shear is shown in Fig. B-2. Again, an HS20 legal load truck was used in the analysis. The vehicle was positioned to induce the maximum shear on the beams.

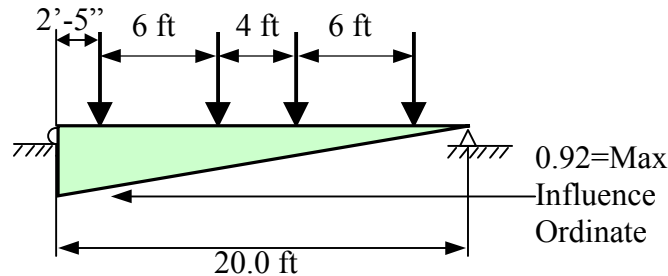


Figure B-2: Truck positioning to induced maximum shear influence in crossbeams (simply supported)

The nominal shear capacity of HCB crossbeams, using the gross concrete section (typical AASHTO or ACI, see ACI 318/95, Eq. 11-3) is,

$$V_c = 2.0(\sqrt{f_c'}) (b_w d) \quad [B-4]$$

The equation assumes that the steel reinforcement did not contribute to shear strength. This assumption was based on the fact that there were no shear stirrups in the beams. A more detailed calculation can be performed, but it is not presented here. For the Horsetail Creek Bridge crossbeams,

$$V_c = (2.0)(\sqrt{2500 \text{ psi}})(12 \text{ in} * 26.0 \text{ in}) = 31,200 \text{ lb}$$

$$V_c = 31.2 \text{ kip}$$

In accordance with Figure B-2, the applied shear load due to live loads (V_{appl}) is as follows:

$$V_{\text{appl}} = (22.5 \text{ kips}) * (0.92 + 0.62 + 0.42 + 0.12) = 46.80 \text{ kips},$$

where: 0.92; 0.62; 0.42 and 0.12 are the shear influence line ordinates under each of the design vehicle axes.

Using this shear capacity, the load rating equation [B-1], the predetermined dead loads (CH2M HILL, 1997) and the associated factors in Table B-1, the rating factor for shear is

or

$$RF_{\text{shear}} = \frac{(0.85) * (31.2 \text{ kip}) - (1.20) * (18.9 \text{ kip})}{(1.033) * (1.30) * (46.8 \text{ kip}) * (1.10)}$$

$$RF_{\text{shear}} = 0.06$$

Since the rating factor is much lower than one, the deficient member requires immediate attention. Such a low rating suggests that the crossbeams should have shown significant distress. However, this is mainly a result of the ultra conservative load rating evaluation procedure adopted by AASHTO and ACI, which does not necessarily represent the real load capacity. Horsetail Creek Bridge did not show any visible signs of structural distress.

Development of Similar beams for testing

Rationale

The mechanical properties of the steel reinforcement used in Horsetail Creek Bridge beams were unknown. It is believed that the steel with which the bridge was constructed has a yield stress of approximately 33 ksi. For bridges constructed before 1959, AASHTO suggests using 33 ksi for the yield strength of the steel reinforcement if the steel cannot be tested (AASHTO, 1994). Current construction methods typically require steel with 60 ksi yield strength. Acquiring steel with yield strength less than 60 ksi is quite difficult. To achieve a 33 ksi yield strength, a special order of steel would have been required, which would have been too expensive for this study. Thus, a reevaluation of the beam strength and serviceability criteria was necessary.

Structural Issues

Regarding reinforced concrete design, there are two important issues of concern: strength and serviceability.

Strength

There are two design philosophies governing the way a member is designed for safety: Load and Resistance Factor Design (LRFD) and Allowable Stress Design (ASD). LRFD emphasizes on adequate prediction of the member strength and factoring the loads along with the predicted strength. This is the predominant design method used for reinforced concrete. ASD uses more strength-of-materials (mechanics) relationships to calculate the stress developed in a member than does LRFD. Prescribed limits of stress are established and the designer must ensure that these stresses are not achieved. LRFD is not currently utilized in the design of FRP strengthened RC beams. However, due to the more realistic and less conservative predictions of the method, LRFD concepts were adopted and adapted to develop design criteria for this study. For development of the full-scale beams, strength criteria were considered important.

Serviceability

Serviceability refers to the day-to-day performance of the structural member and must be assured at service load levels, not at ultimate strength. Prescribed limits are established, such as maximum permissible crack widths and deflections. Due to the nature of the conducted experiments, serviceability was not a major concern in designing the full-scale beams.

Horsetail Creek Bridge Beams Prior to Strengthening

There are two types of primary bending elements in HCB: crossbeams (orthogonal to traffic) and longitudinal beams (parallel to traffic). Prior to strengthening, the only structural difference between the two beam types was that the crossbeams had one more 1 in² flexural rebar than the longitudinal beams. Consequently, the crossbeams had a slightly higher capacity in bending. Load rating showed the crossbeams had a lower shear rating factor. For this reason, the experimental beams were designed after the crossbeams. The beam dimensions and steel reinforcement positions for the crossbeams are shown in Figures 2-1 and 2-2. There were no shear steel stirrups, which are now required by current standards¹.

Matching Moment Capacity

The critical section for any flexural loading of the beam is likely to be near the midspan². In an effort to keep the full-size beams as close to the original as possible, the number of steel reinforcement bars and locations, the estimated concrete strength, and the beam dimensions remained the same. The only parameter that was changed in order to match capacity with the original beam was the cross-sectional area of the flexural steel reinforcement. The calculations for determining the required steel cross-sectional area are given below. These calculations neglect the 5/8-in square bars near the top, which were found have little affect.

The moment capacity, M_n , was approximately

$$M_n = A_s f_y (d - a/2) \quad [B-5]$$

where “a” is the equivalent rectangular Whitney stress block (Whitney, 1956). This condition is only true, provided the steel yields before the concrete crushes at the top compression fibers. The balance steel ratio, ρ_b , is the ratio where simultaneous yielding of the steel and crushing of the concrete occurs (Nilson, 1997). For the pre-strengthened HCB beams,

$$\rho_b = 0.85 \beta_1 \frac{f_c'}{f_y} \frac{87,000}{87,000 + f_y} \quad [B-6]$$

If the steel ratio of the beam is lower than this value, yielding of the tension steel precedes crushing of the concrete. Hence,

$$\rho_b = 0.85 (0.85) \frac{2500}{33,000} \frac{87,000}{33,000 + 33,000} = 0.0397$$

$$\rho = A_s / bd = 5.00 \text{ in}^2 / (12 \text{ in} * 28 \text{ in}) = 0.0149$$

¹ Design of reinforced concrete bridges is specified by the AASHTO Guide Specifications for Highway Bridges, 16th Edition.

² Midspan refers to the section at the geometric center between two support points, that is ½ the span length.

Since the steel ratio was below the balanced ratio, the steel yields first. For the pre-strengthened HCB beams, the equivalent stress block “a” was approximated by

$$a = \frac{A_s f_y}{0.85 f_c' b} \quad [B-7]$$

$$a = \frac{(5.00 \text{ in}^2)(33 \text{ ksi})}{(0.85)(2.5 \text{ ksi})(12 \text{ in})} = 6.471 \text{ in}$$

Then, from equation [B-2]

$$M_n = (5.00 \text{ in}^2)(33 \text{ ksi})(28 - 6.471/2) = 4086 \text{ kip-in}$$

$$M_n = 341 \text{ kip-ft}$$

Since the geometry of the beam was to be retained as closely as possible, the area of steel was reduced to offset the increased yield strength. To do this, the tension force developed in the steel reinforcement was matched, such that

$$A_s f_y = (5 \text{ in}^2)(33 \text{ ksi}) = 165 \text{ kip} \quad [B-8]$$

Since the full-size beams were to be made using steel with $f_y = 60 \text{ ksi}$ then,

$$A_{s, \text{new}} = 165 \text{ kip} / 60 \text{ ksi} = 2.75 \text{ in}^2$$

Since steel reinforcing is fabricated in specific sizes, a reasonable combination of five bars in the same location was needed. Two #6 rebar and three #7 rebar provided a steel area of 2.68 in^2 . Using this combination of reinforcement, the new moment capacity was calculated by,

$$a = \frac{(2.68 \text{ in}^2)(60 \text{ ksi})}{(0.85)(2.5 \text{ ksi})(12 \text{ in})} = 6.306 \text{ in}$$

$$M_n = (2.68 \text{ in}^2)(60 \text{ ksi})(27.75 - 6.306/2) = 3955 \text{ kip-in}$$

$$M_n = 330 \text{ kip-ft}$$

References

American Association of State and Highway Transportation Officials (AASHTO), 1994 Manual for Condition Evaluation of Bridges.

American Association of State and Highway Transportation Officials (AASHTO), 1989. Guide Specifications for Strength Evaluation of Existing Steel and Concrete Bridges.

American Concrete Institute (ACI), 1995. Building Code and Commentary for Structural Concrete Design, ACI, Place of Publication.

CH2M HILL and TAMS Consultants, 1997. Load Rating Calculation Book No. 9090 for Horsetail Creek Bridge No. 04543. Contact: CH2M HILL, Inc., 2300 NW Walnut Blvd, Corvallis, Oregon 97330.

Nilson, A.H., 1997. Design of Concrete Structures, 12th Edition, McGraw-Hill: New York.

Whitney, C.S., and E. Cohen, 1957. "Guide for Ultimate Strength Design of Reinforced Concrete," *Journal of the American Concrete Institute*, ACI, Title No. 53-25, June, 1957.

Notation

Table B-2: Appendix B Notation

Variable	Description	US Standard Units [†]	Metric Units [†]
a	Equivalent Whitney stress block depth converted from the depth to the neutral axis	in	mm
A _s	Area of primary tension reinforcing steel	in ²	mm ²
A _{s,new}	New area of primary tension reinforcing steel, converted for new tension reinforcement	in ²	mm ²
b	Compression flange/block width	in	mm
b _w	Web width of the beam	in	mm
d	Structural depth of the primary steel reinforcing from the top compression fibers in the beam	in	mm
DF	Distribution factor which accounts for wheel distribution per lane. In this analysis, these are influence ordinates.	~	~
DL, LL	Maximum applied dead and live load, respectively	Varies	Varies
f _c '	28-day specified compressive strength of the concrete	psi	kPa
f _y	Steel reinforcing yield stress	ksi	MPa
I	Impact factor	~	~
M _n	Nominal moment capacity	kip-ft	kN-m
RF	rating factor of the structural element	~	~
RF _{flexure}	Rating factor in flexure	~	~
R _n	General nominal structural capacity	~	~
V _c	Shear capacity of the concrete section	kip	kN
V _n	Nominal shear capacity	kip	kN
V _s	Shear capacity of the steel stirrups	kip	kN
β ₁		~	~
φ	Strength reduction factor	~	~
γ _{DL} , γ _{LL}	Dead and live load factors, respectively	~	~
ρ _b	Balance steel ratio where simultaneous crushing of the concrete would occur with yielding of the tension steel.	~	~

[†] Typical units presented. The use of “~” implies the variable has no units.

APPENDIX C: EXPERIMENTAL DATA

APPENDIX C: EXPERIMENTAL DATA

List of Figures

Figure C-1. Control Beam deflection characteristics	2
Figure C-2. Control Beam strain at 1067 mm from beam end.....	3
Figure C-3. Control Beam strain at 1500 mm from beam end.....	3
Figure C-4. Control Beam compressive strain comparison.....	4
Figure C-5. Control Beam tensile strain comparison.....	4
Figure C-6. Control Beam evidence of shear crack formation.....	5
Figure C-7. Control Beam failure by shear crack formation	5
Figure C-8. Flexure-Only Beam deflection characteristics	6
Figure C-9. Flexure-Only Beam strain 1067 mm from beam end	6
Figure C-10. Flexure-Only Beam strain 1500 mm from beam end	7
Figure C-11. Flexure-Only Beam compressive strain comparison	7
Figure C-12. Flexure-Only Beam tensile strain comparison	8
Figure C-13. Flexure-Only Beam early tensile strain comparison	8
Figure C-14. Flexure-Only Beam strain for comparison with fiber optic strain gauges	9
Figure C-15. Flexure-Only Beam evidence of shear crack formation	9
Figure C-16. Flexure-Only Beam failure by shear crack formation.....	10
Figure C-16. Shear-Only Beam deflection characteristics	10
Figure C-17. Shear-Only Beam strain 1067 mm from beam end	11
Figure C-18. Shear-Only Beam strain 1500 mm from beam end	11
Figure C-19. Shear-only beam compressive strain comparison.....	12
Figure C-20. Shear-Only Beam tensile strain comparison	12
Figure C-21. Shear-Only Beam yielding of tension reinforcing steel	13
Figure C-22. Shear-Only Beam failure: steel yields and concrete crushes	13
Figure C-23. S&F Beam deflection characteristics	14
Figure C-24. S&F Beam strain 1067 mm from beam end	14
Figure C-25. S&F Beam strain 1500 mm from beam end	15
Figure C-26. S&F Beam compressive strain comparison.....	15
Figure C-27. S&F Beam tensile strain comparison.....	16
Figure C-28. Common resistance strain gauge locations (dimensions in mm)	20
Figure C-29. Gauge type comparison—S&F Beam	20
Figure C-30. Strain from flexural fiber optic strain gauges—S&F Beam	21
Figure C-31. Strain from shear fiber optic strain gauges embedded in concrete—S&F Beam	21
Figure C-32. Comparison of shear fiber optic strain gauges embedded in concrete and on top of the FRP reinforcement—S&F beam.....	22
Figure C-33. Fiber optic strain gauge locations (dimensions in mm)	23
Figure C-34. Control Beam cracking (a) and crack responsible for failure (b)	24
Figure C-35. Diagonal tension crack responsible for failure of F-Only Beam.....	25
Figure C-36. S-Only Beam (a) and flexural cracks (darkened for contrast) in GFRP near ultimate load (b) .	25
Figure C-37. Comparison of beam cracking (dimensions in mm)	26
Figure C-38. Fiber optic vs. resistance strain gauge comparison—F-Only Beam.....	29
Figure C-39. Principal compression stress trajectories for a homogeneous simple beam uniformly loaded (after Nilson, 1997)	29

List of Tables

Table C-1 Resistance strain gauge identification	16
Table C-2. Fiber optic strain gauge identification.....	22

NOTE: Figures C-1 to C-27 show deflection and strain results. Table C-1, in conjunction with Figure C-28, provides a key to the strain gauge labels. Figures C-29 to C-32 show the results from the fiber optic strain gauges. Table C-2, in conjunction with Figure C-33, provides a key to the fiber optic strain gauge labels. The strain gauge data is followed by a discussion of the fiber optic strain gauge data and an analysis of the crack patterns.

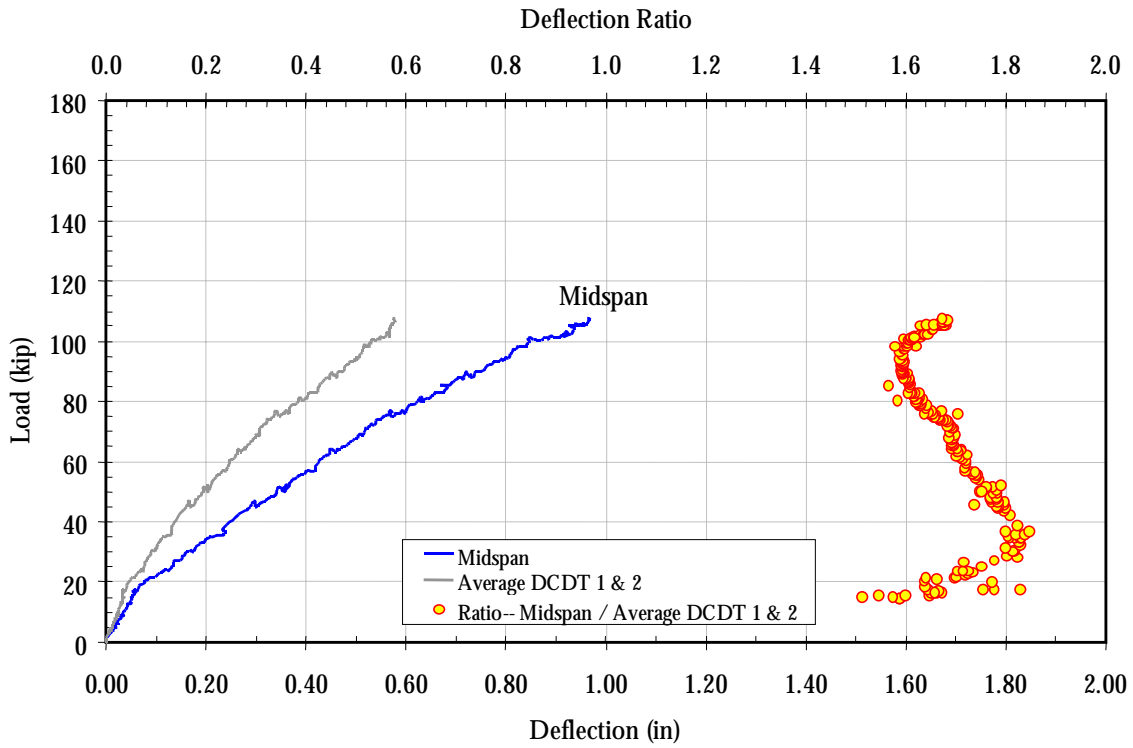


Figure C-1: Control Beam deflection characteristics

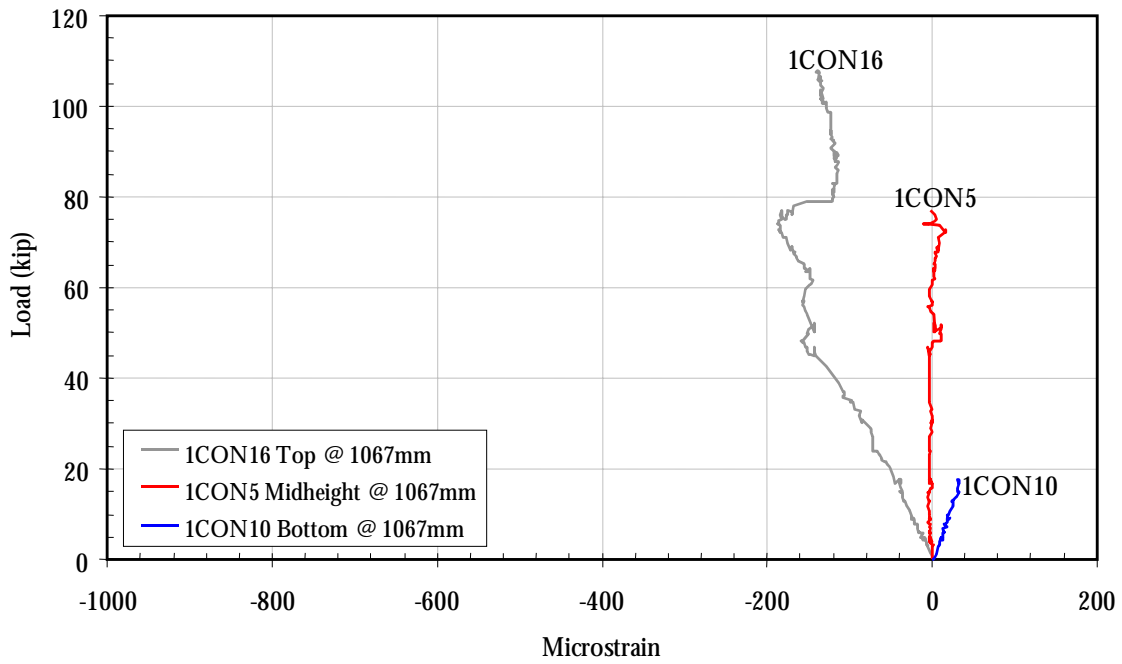


Figure C-2: Control Beam strain at 1067 mm from beam end

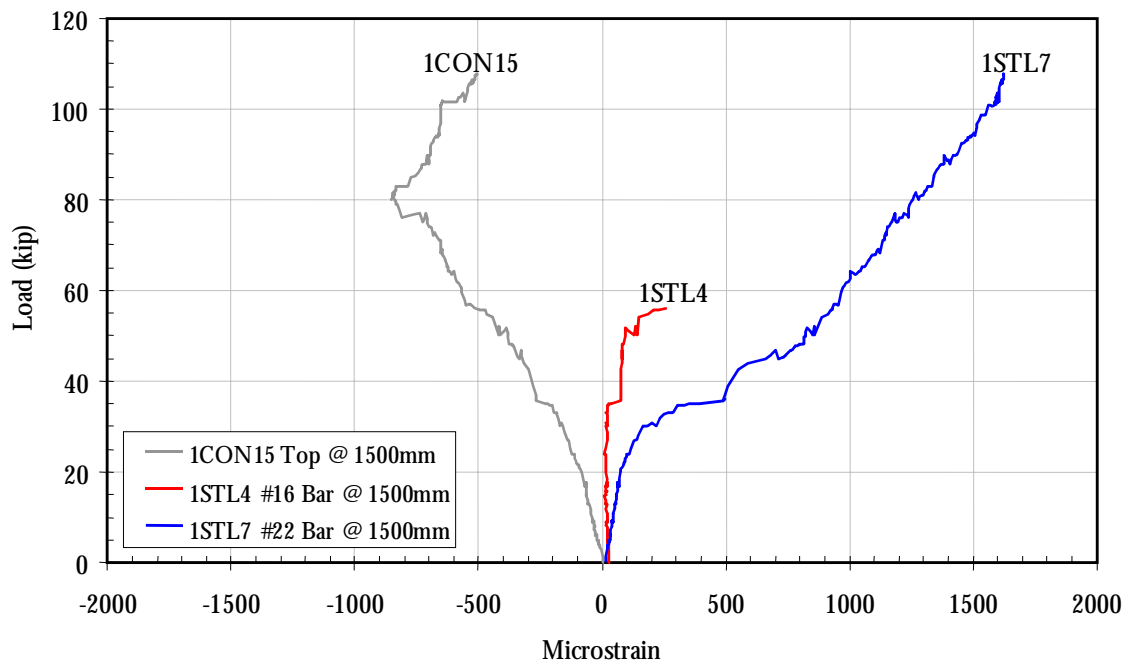


Figure C-3: Control Beam strain at 1500 mm from beam end

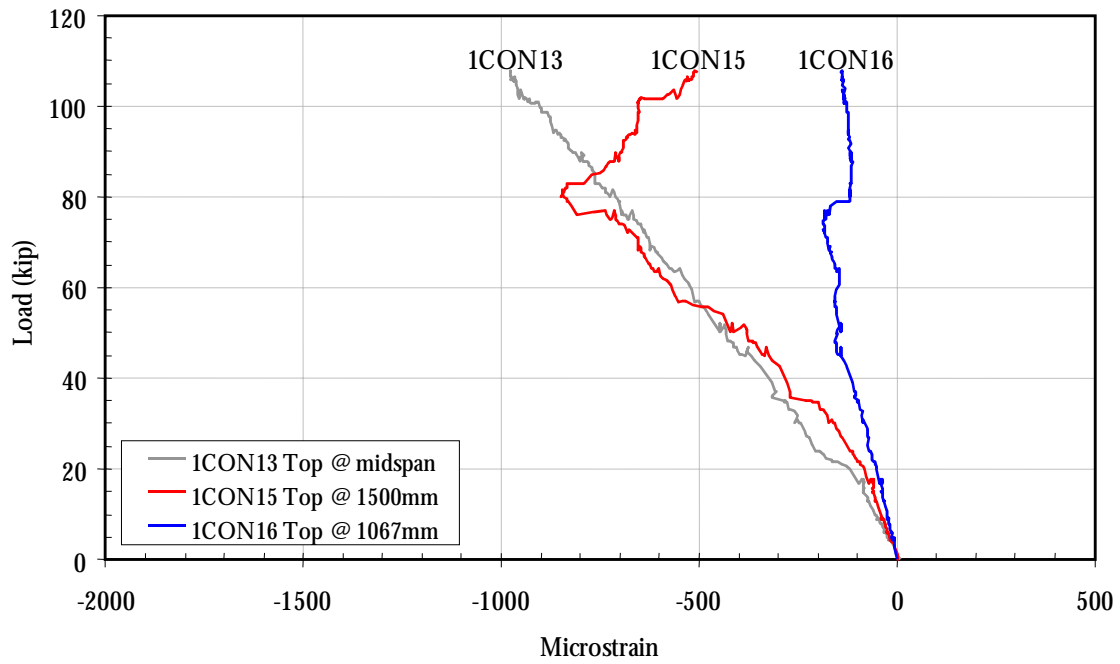


Figure C-4: Control Beam compressive strain comparison

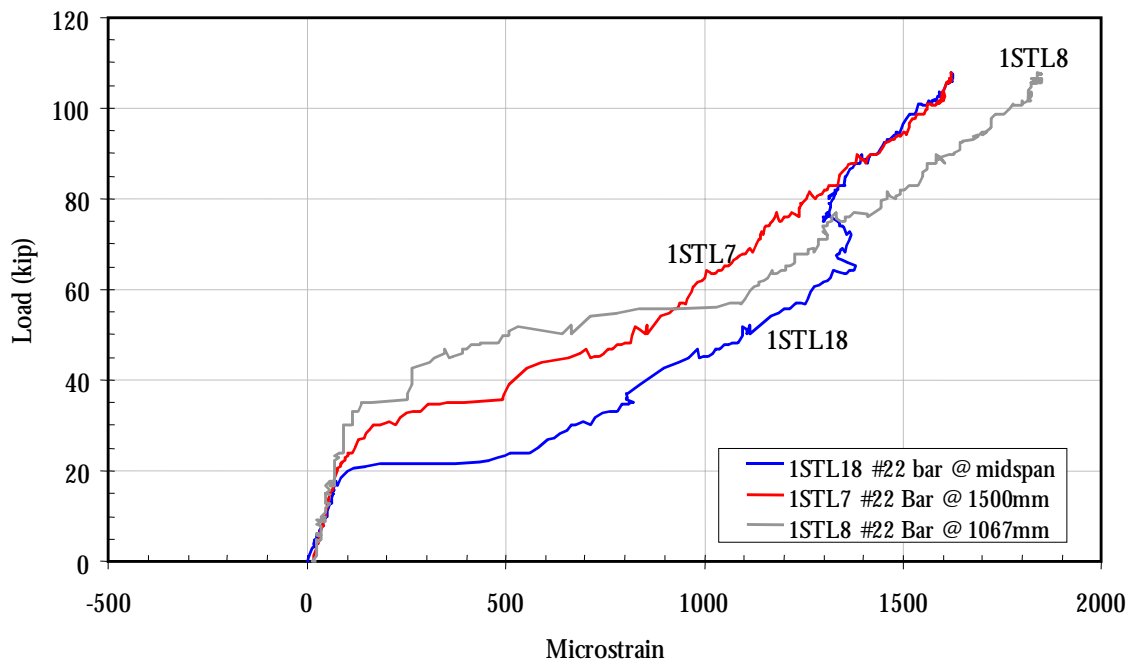


Figure C-5: Control Beam tensile strain comparison

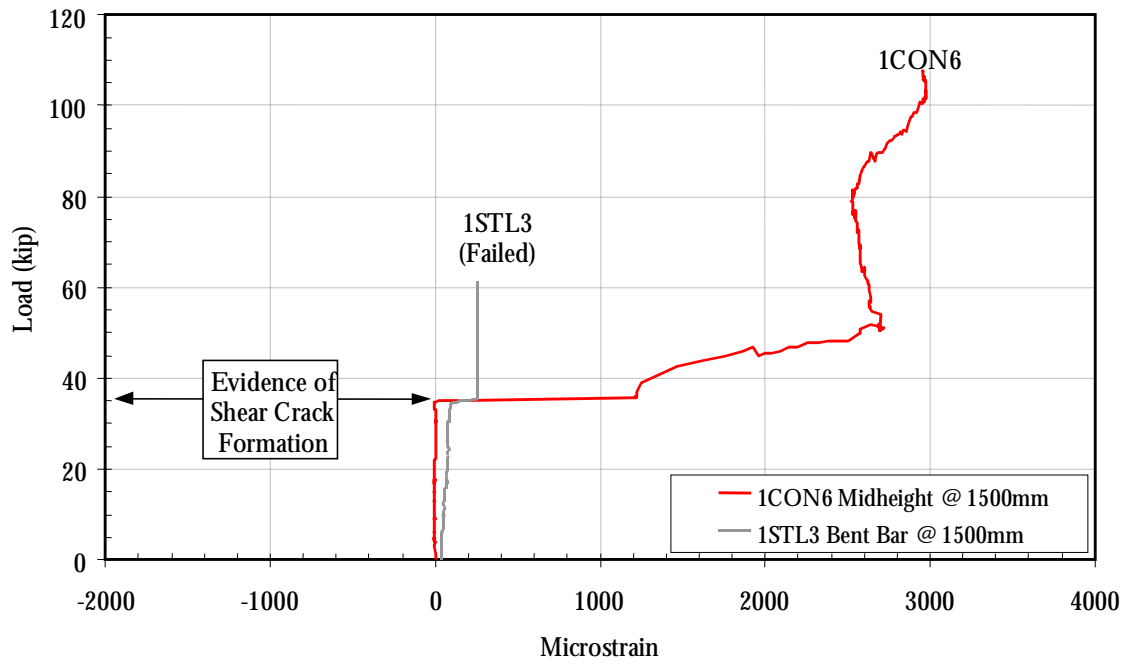


Figure C-6: Control Beam evidence of shear crack formation

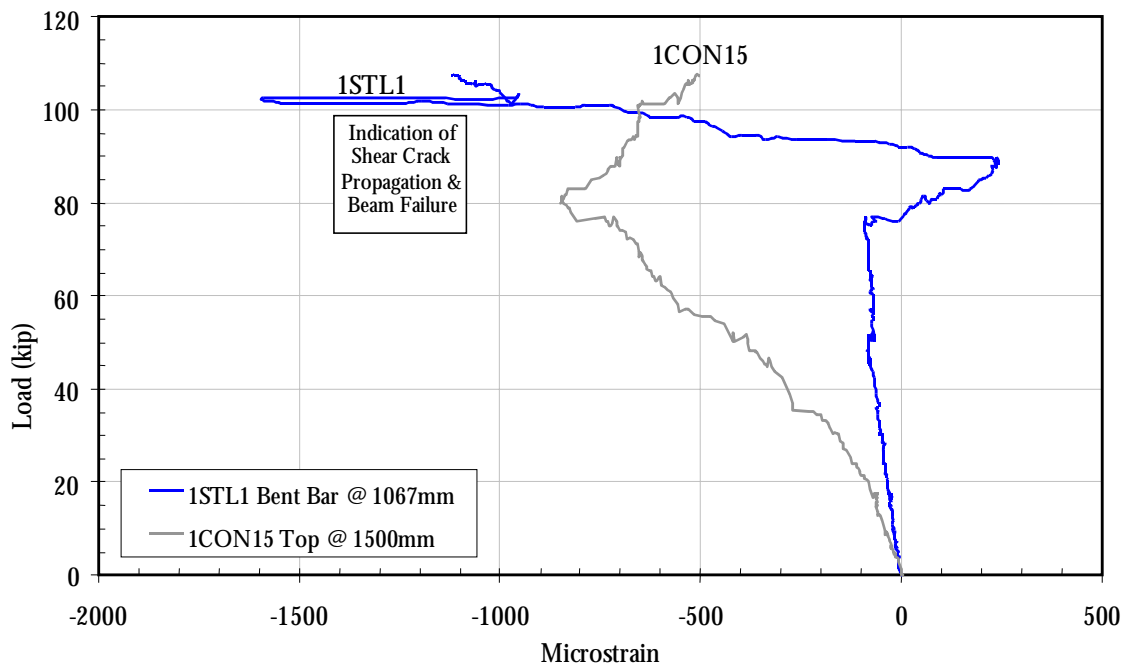


Figure C-7: Control Beam failure by shear crack formation

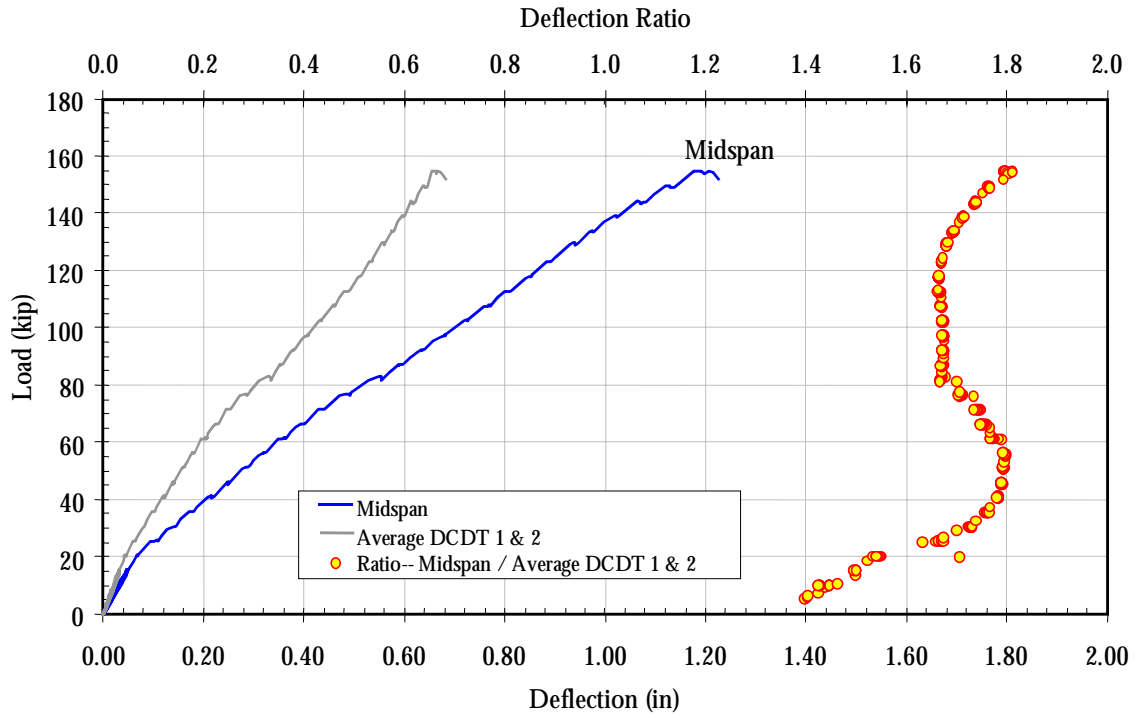


Figure C-8: Flexure-Only Beam deflection characteristics

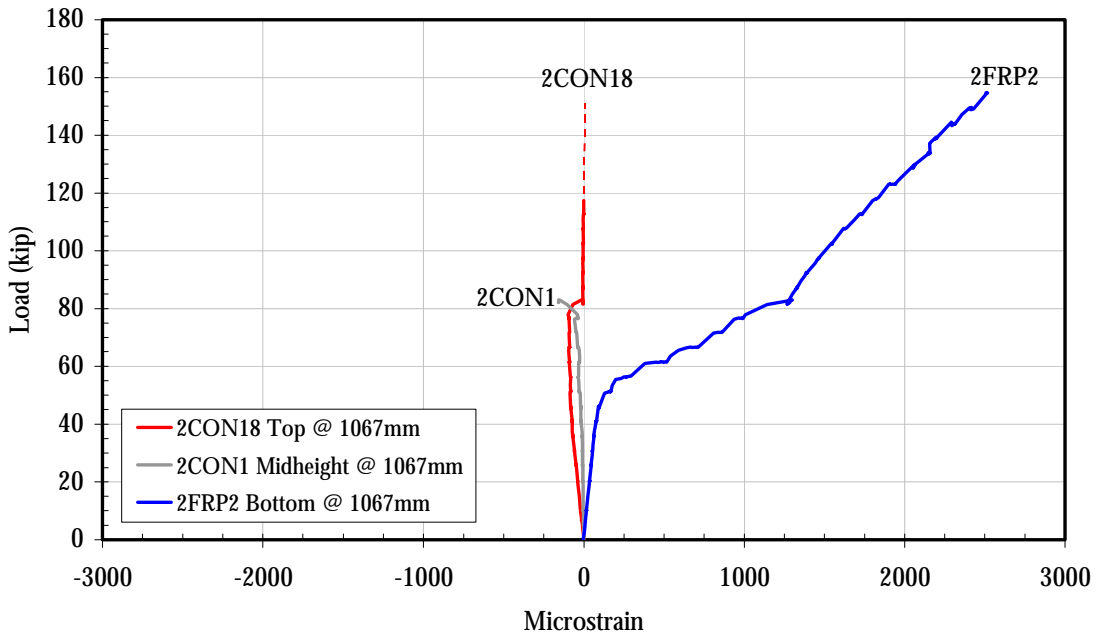


Figure C-9: Flexure-Only Beam strain 1067 mm from beam end

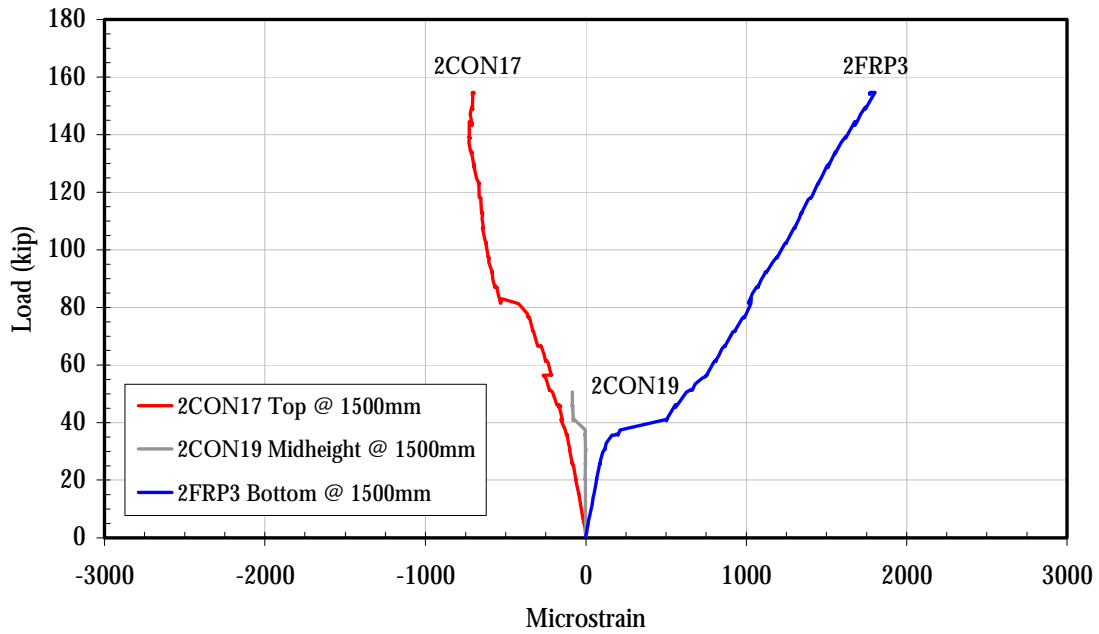


Figure C-10: Flexure-Only Beam strain 1500 mm from beam end

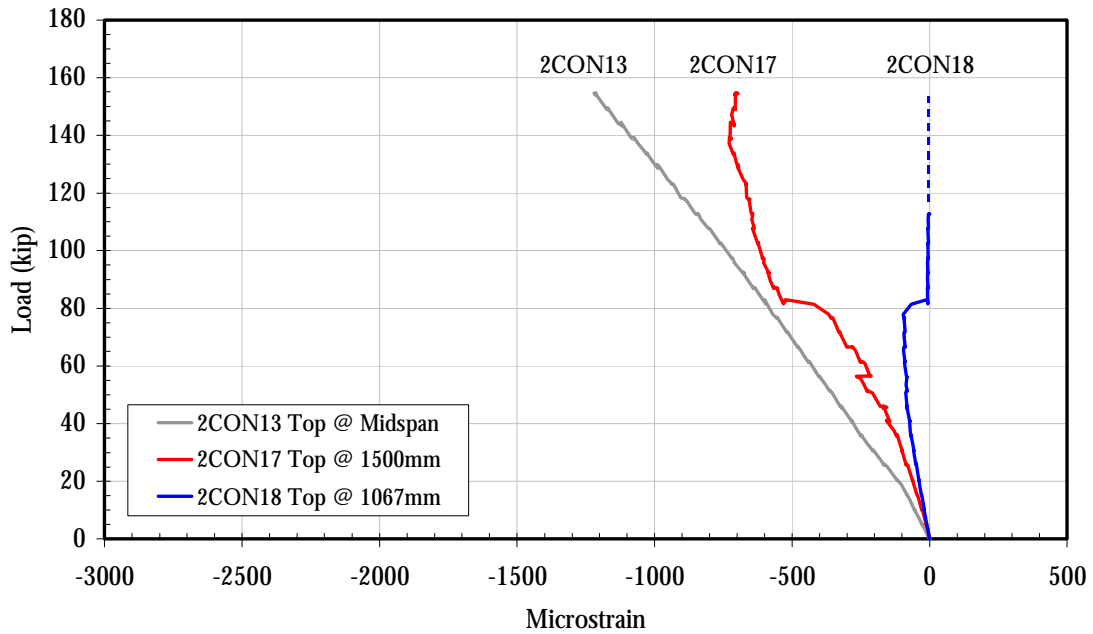


Figure C-11: Flexure-Only Beam compressive strain comparison

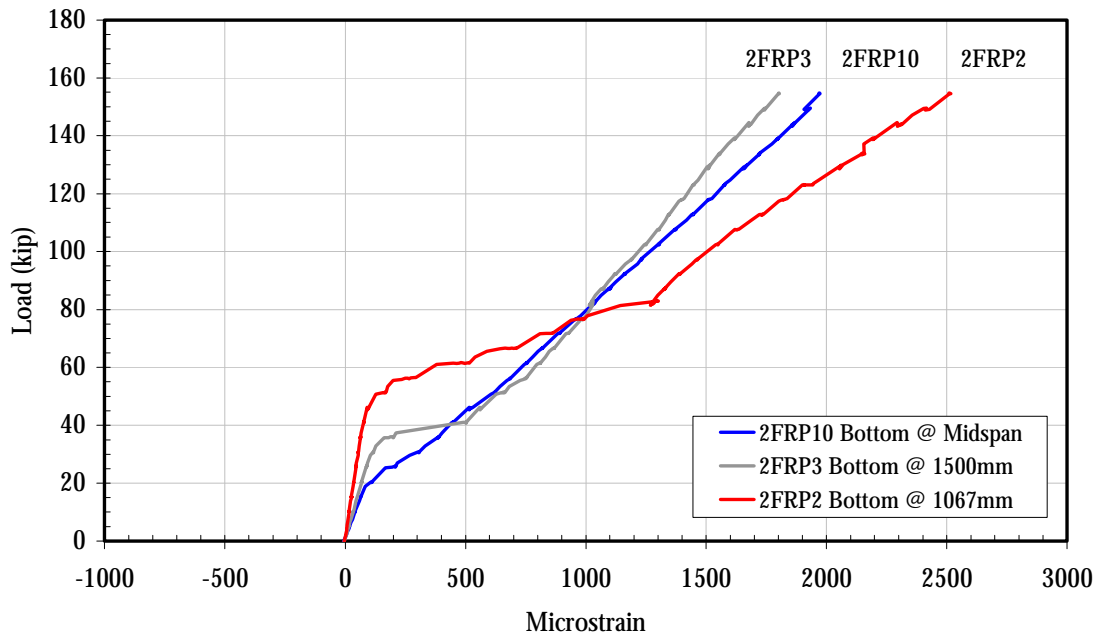


Figure C-12: Flexure-Only Beam tensile strain comparison

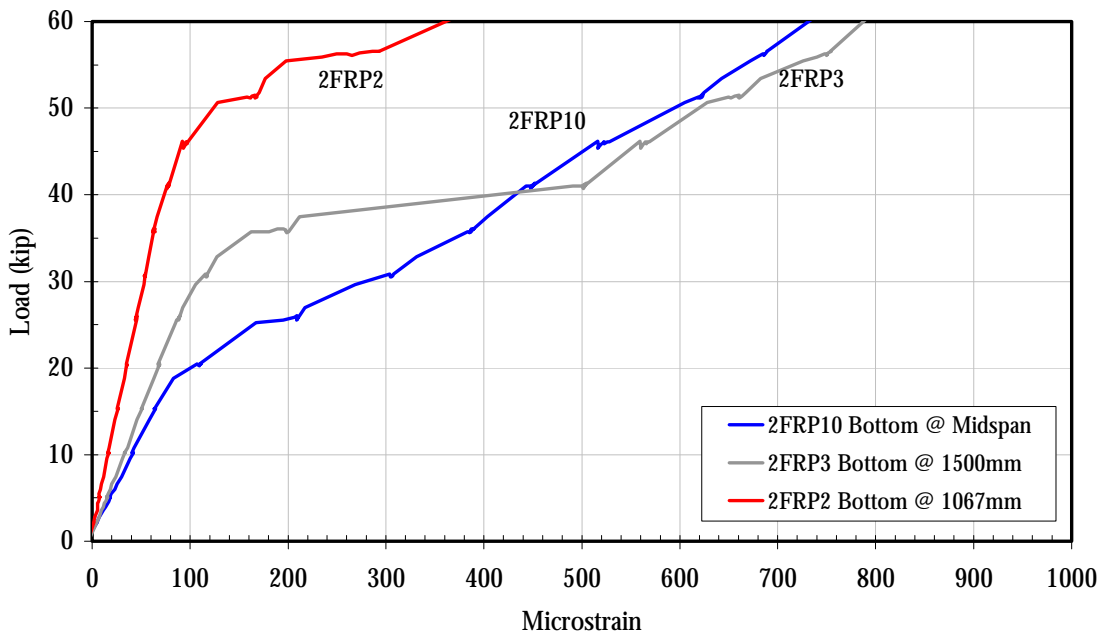


Figure C-13: Flexure-Only Beam early tensile strain comparison

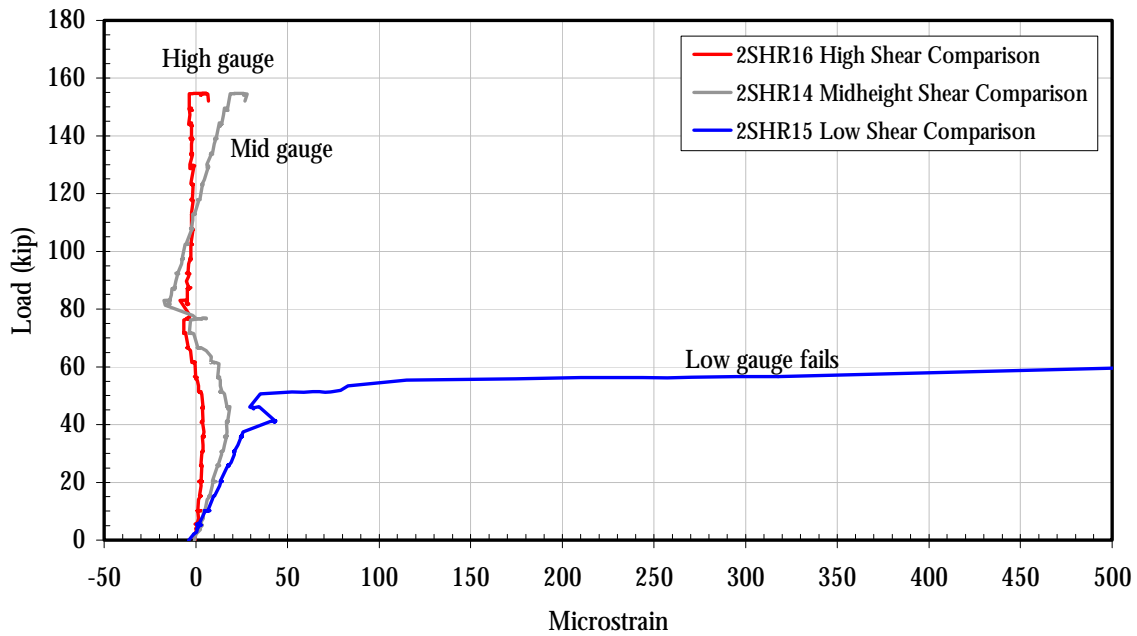


Figure C-14: Flexure-Only Beam strain for comparison with fiber optic strain gauges

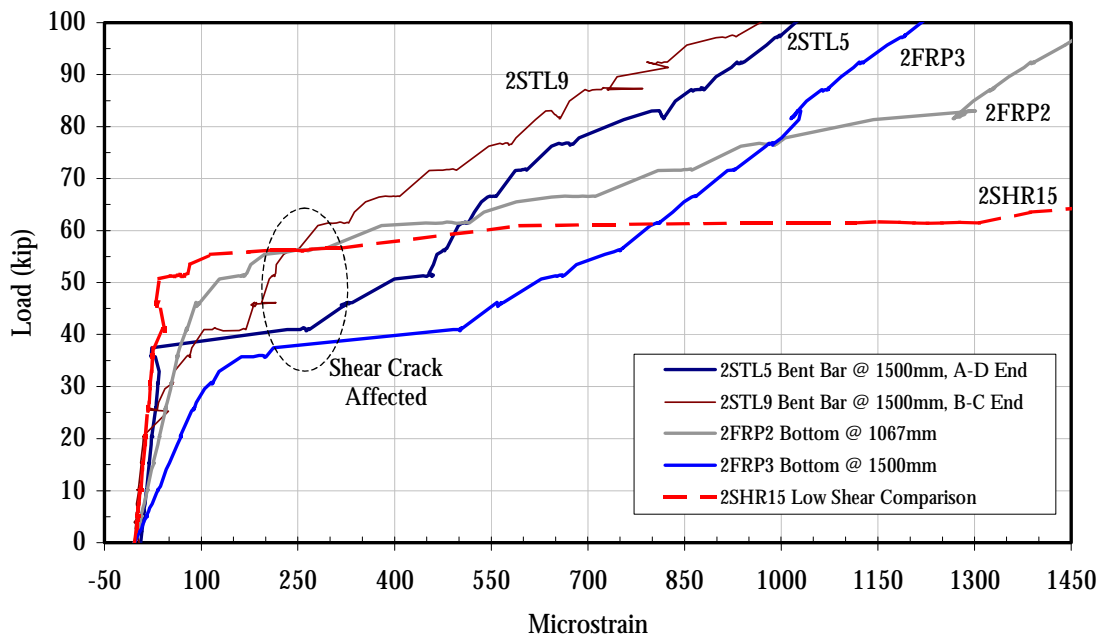


Figure C-15: Flexure-Only Beam evidence of shear crack formation

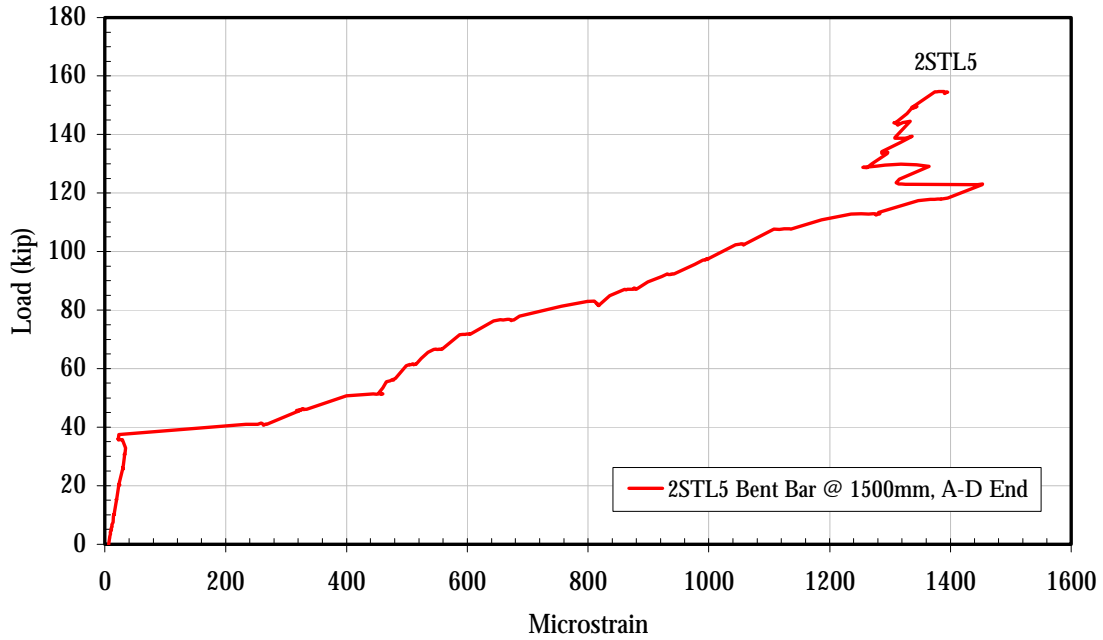


Figure C-16: Flexure-Only Beam failure by shear crack formation

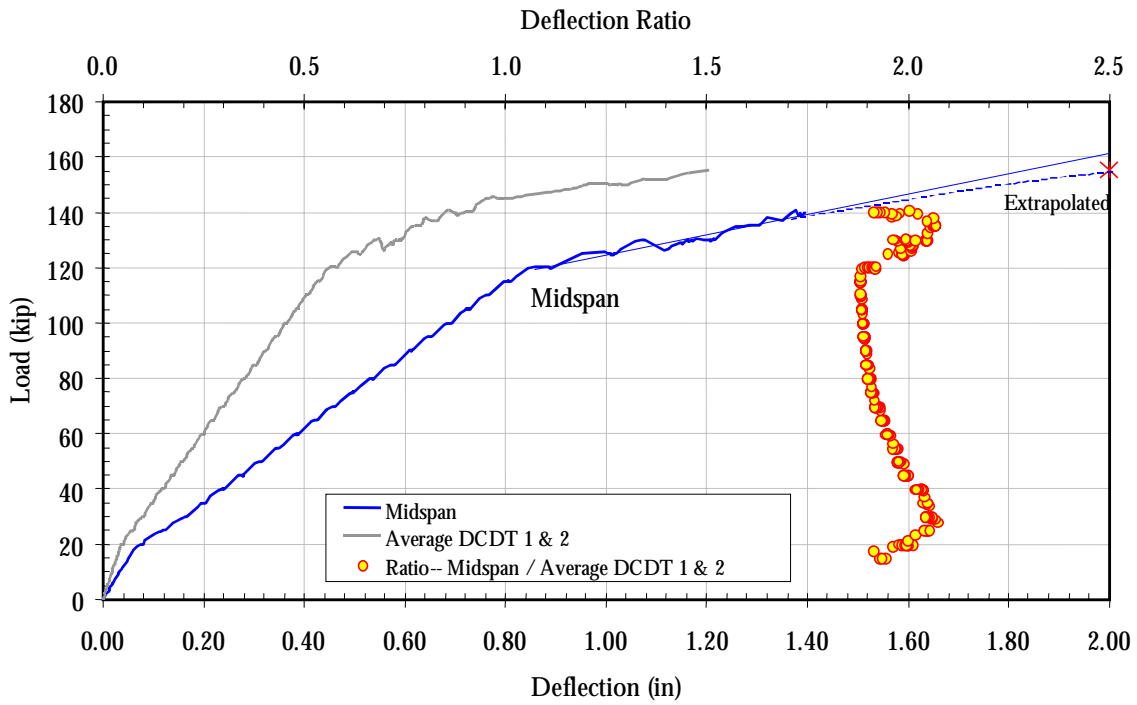


Figure C-16: Shear-Only Beam deflection characteristics

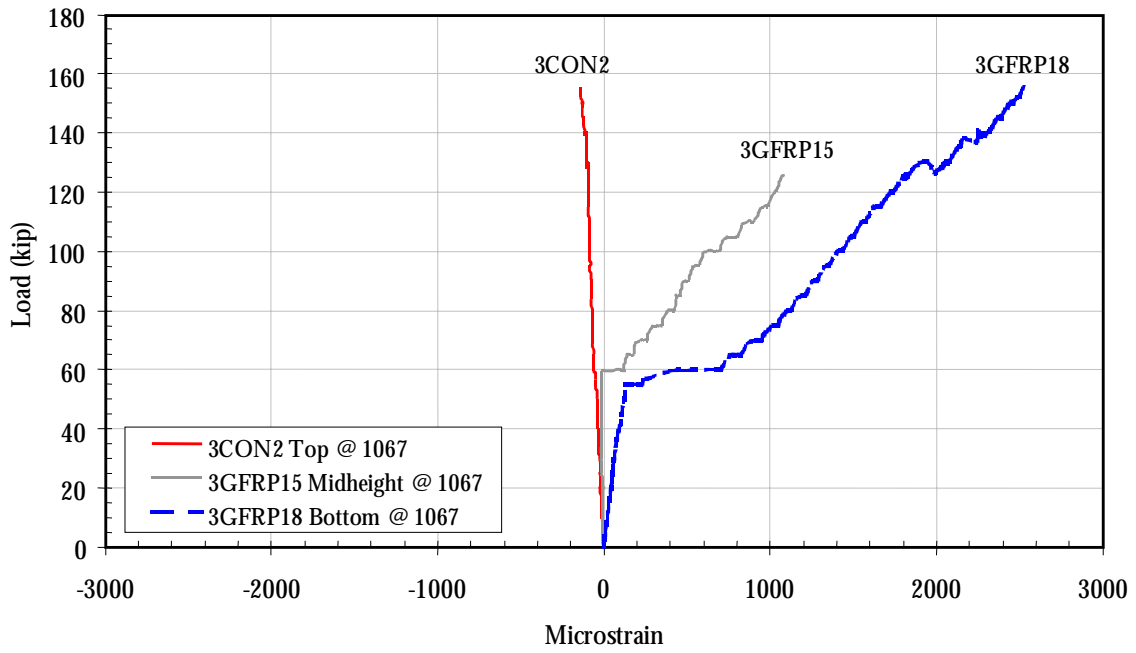


Figure C-17: Shear-Only Beam strain 1067 mm from beam end

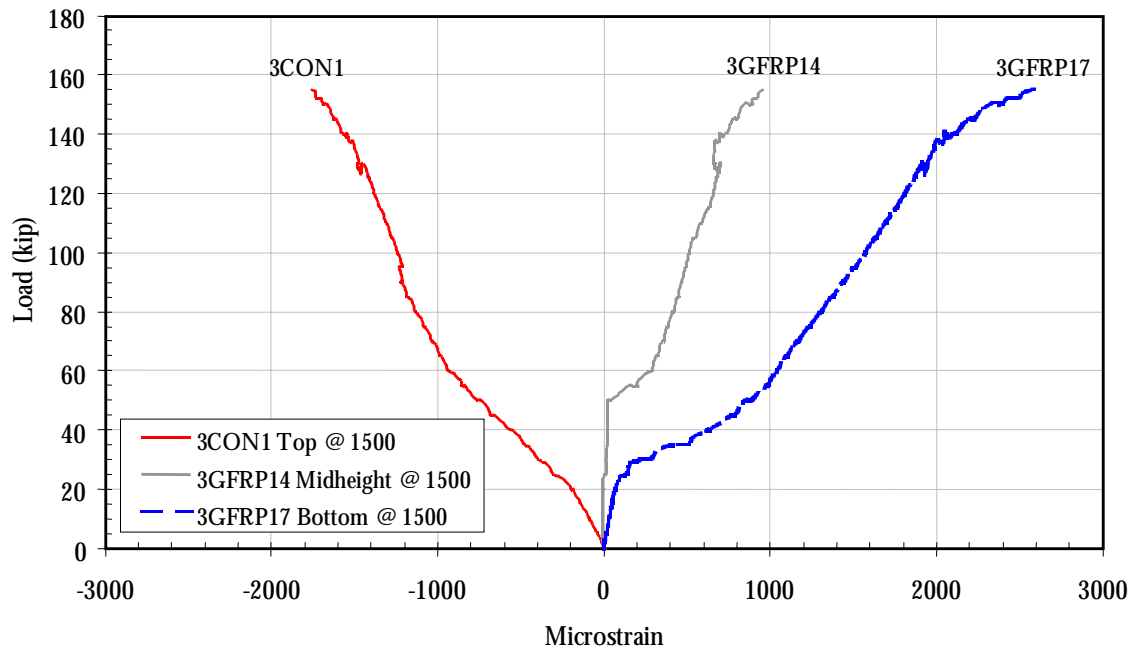


Figure C-18: Shear-Only Beam strain 1500 mm from beam end

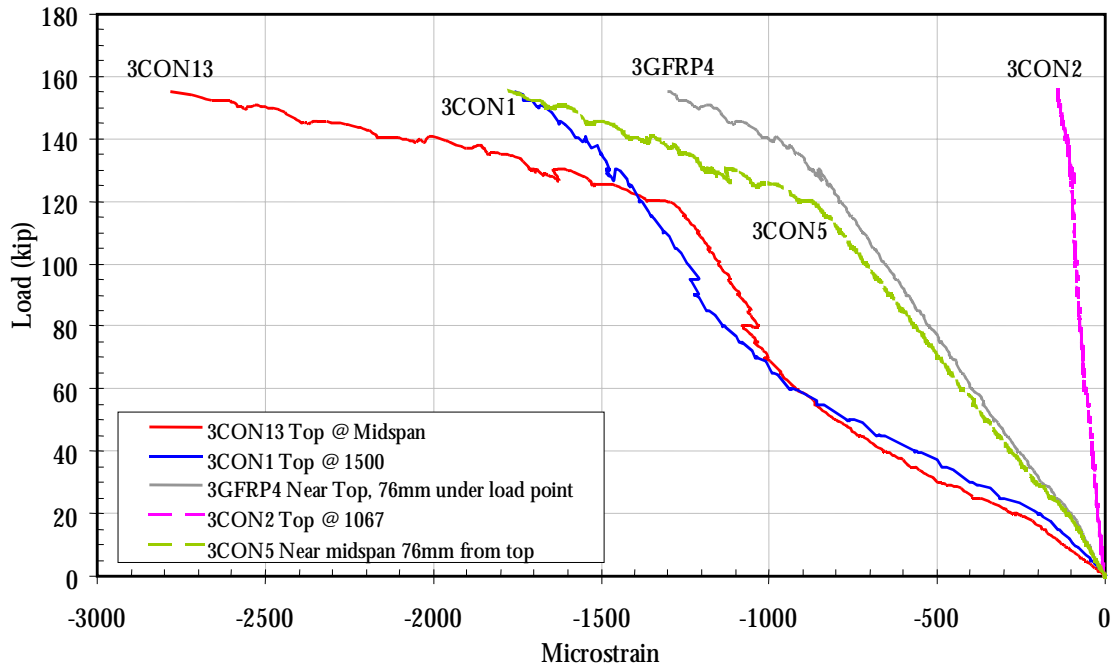


Figure C-19: Shear-only beam compressive strain comparison

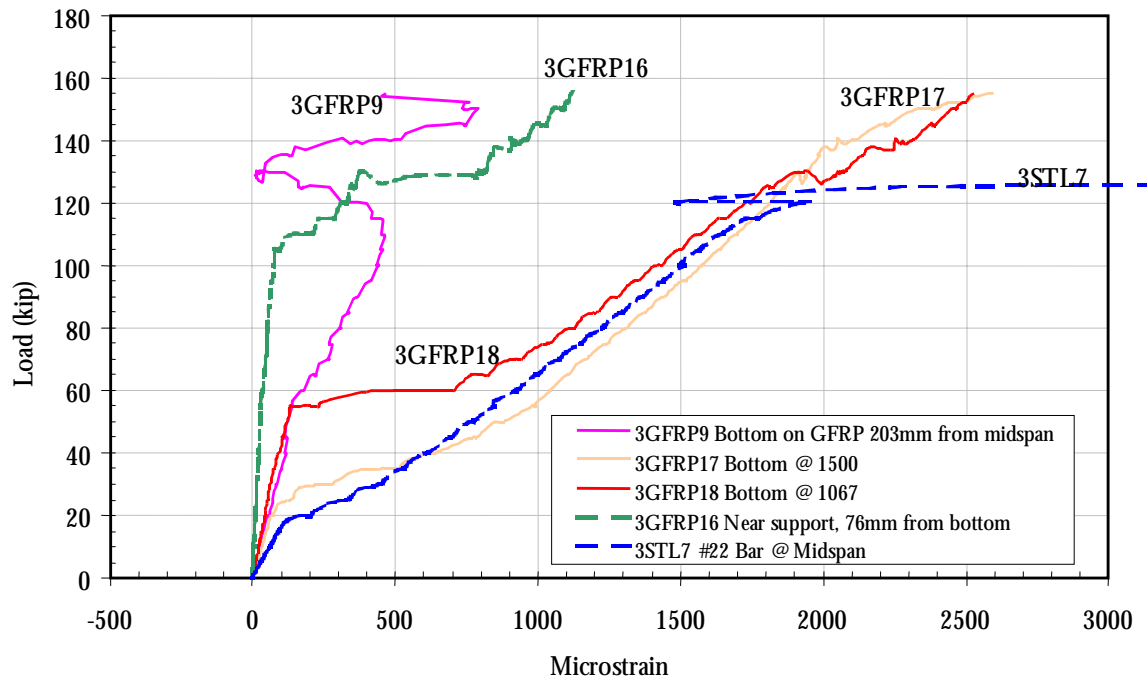


Figure C-20: Shear-Only Beam tensile strain comparison

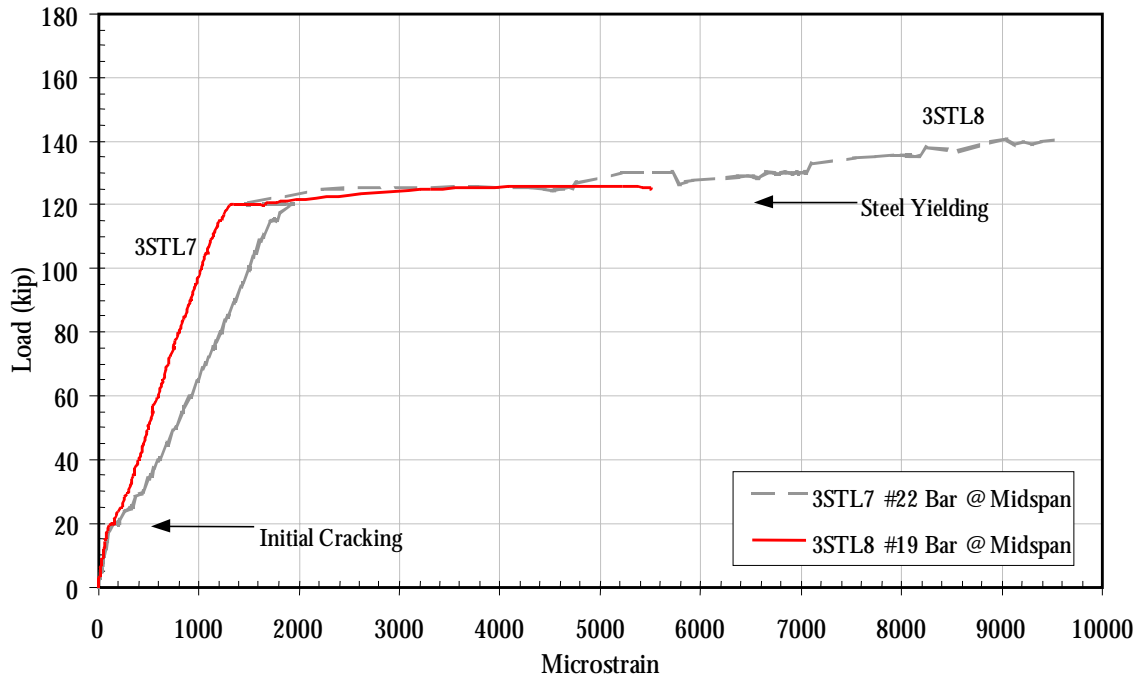


Figure C-21: Shear-Only Beam yielding of tension reinforcing steel

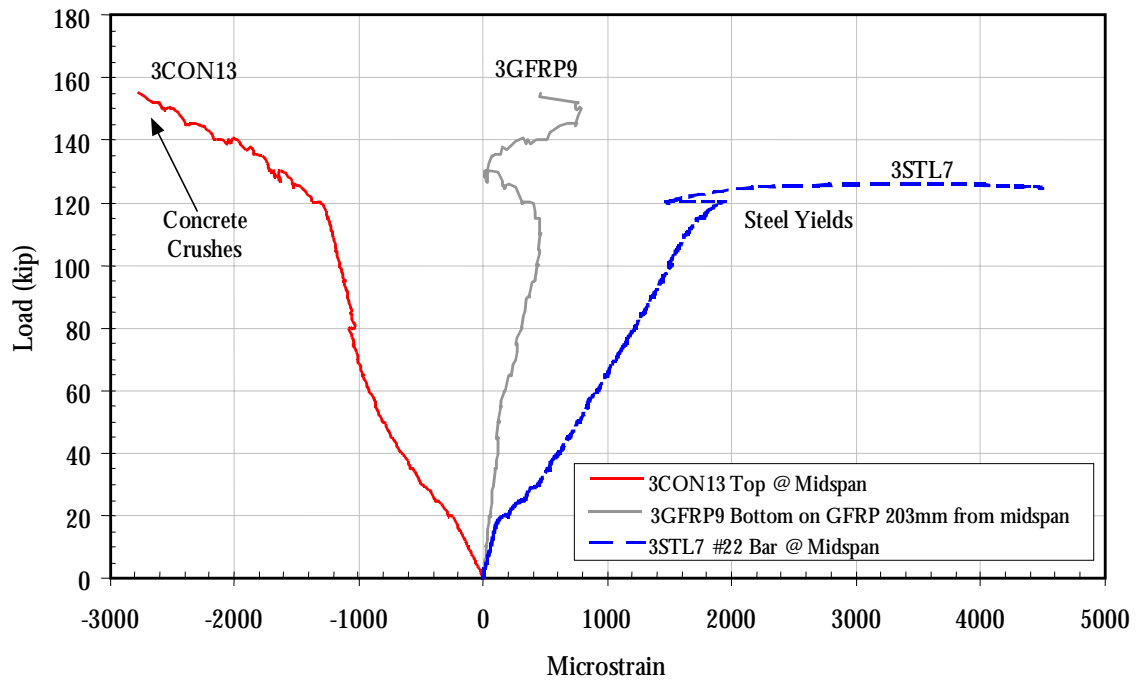


Figure C-22: Shear-Only Beam failure: steel yields and concrete crushes

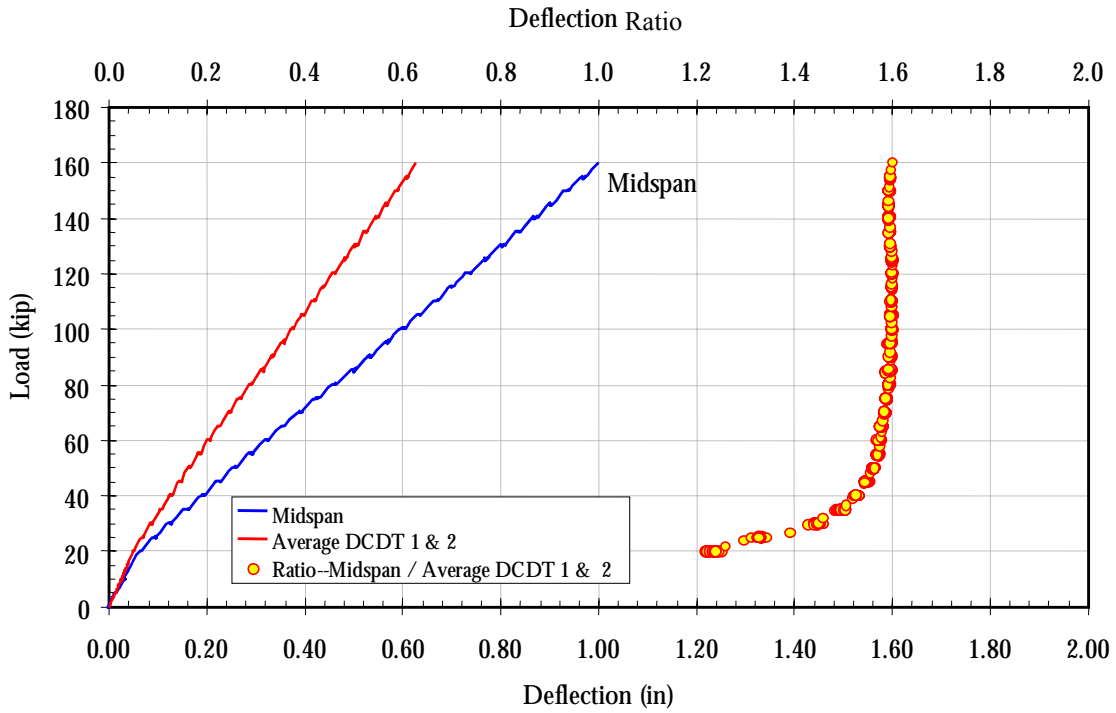


Figure C-23: S&F Beam deflection characteristics

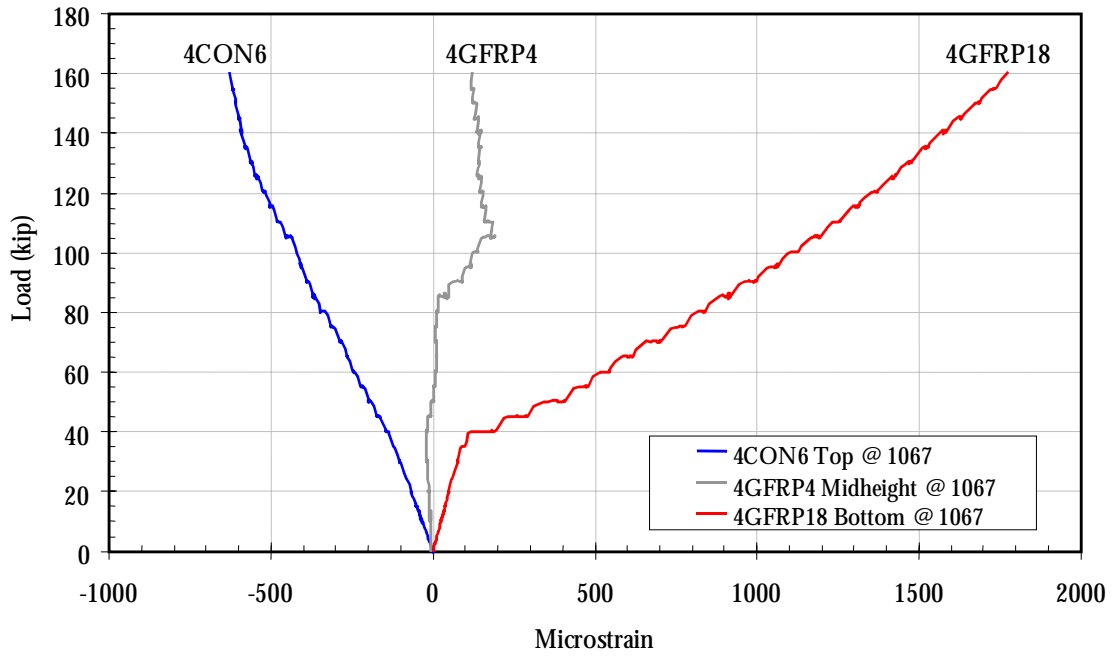


Figure C-24: S&F Beam strain 1067 mm from beam end

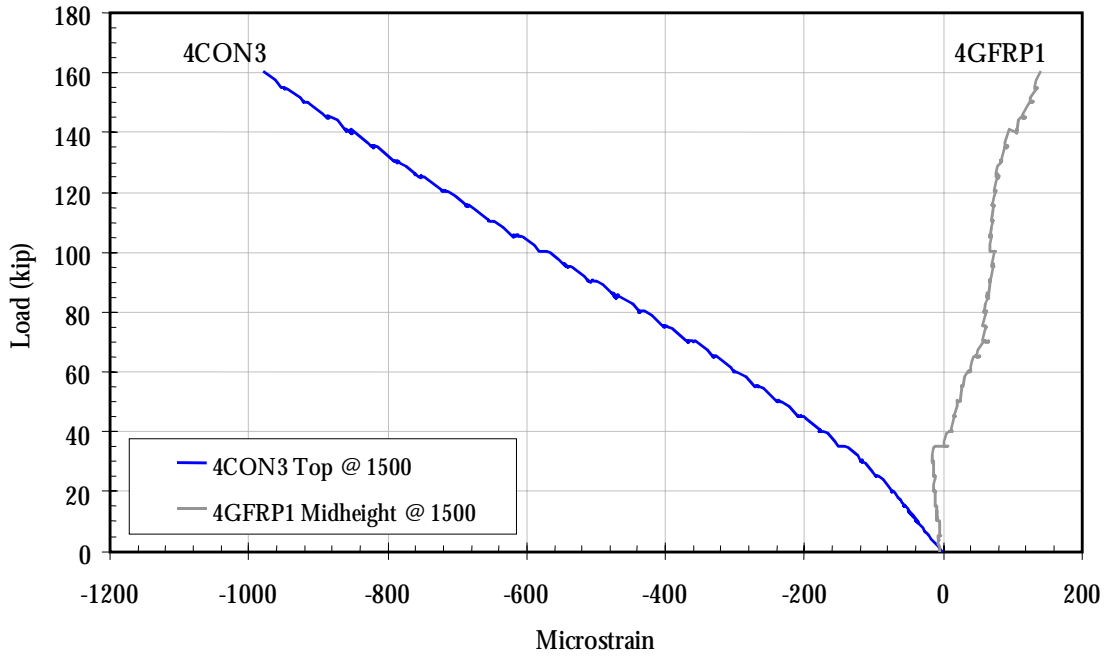


Figure C-25: S&F Beam strain 1500 mm from beam end

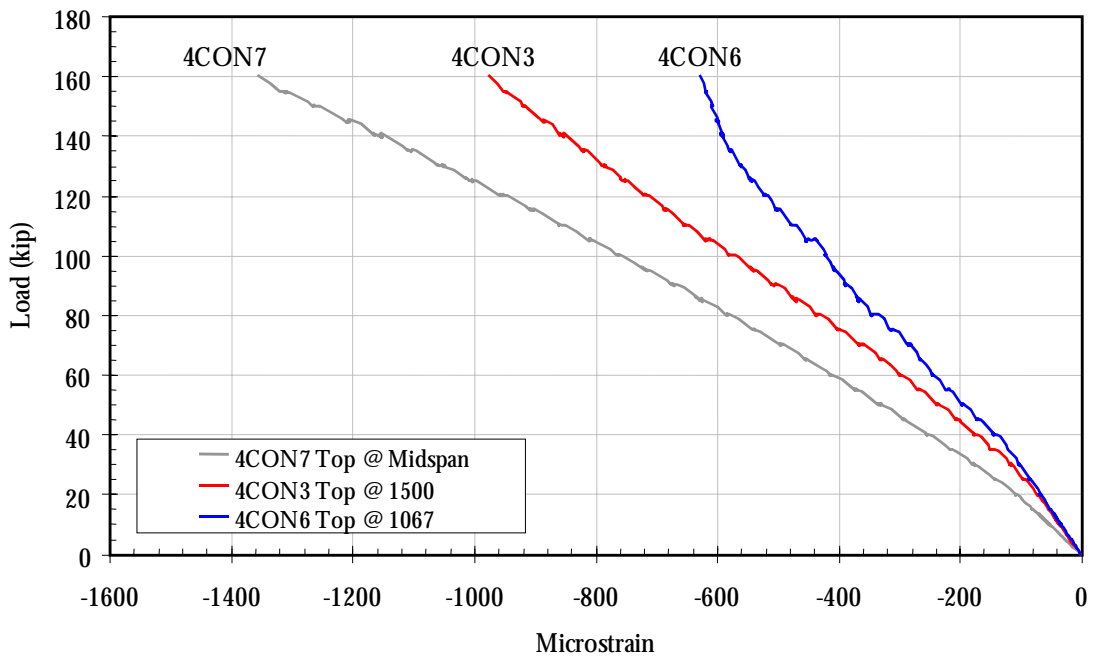


Figure C-26: S&F Beam compressive strain comparison

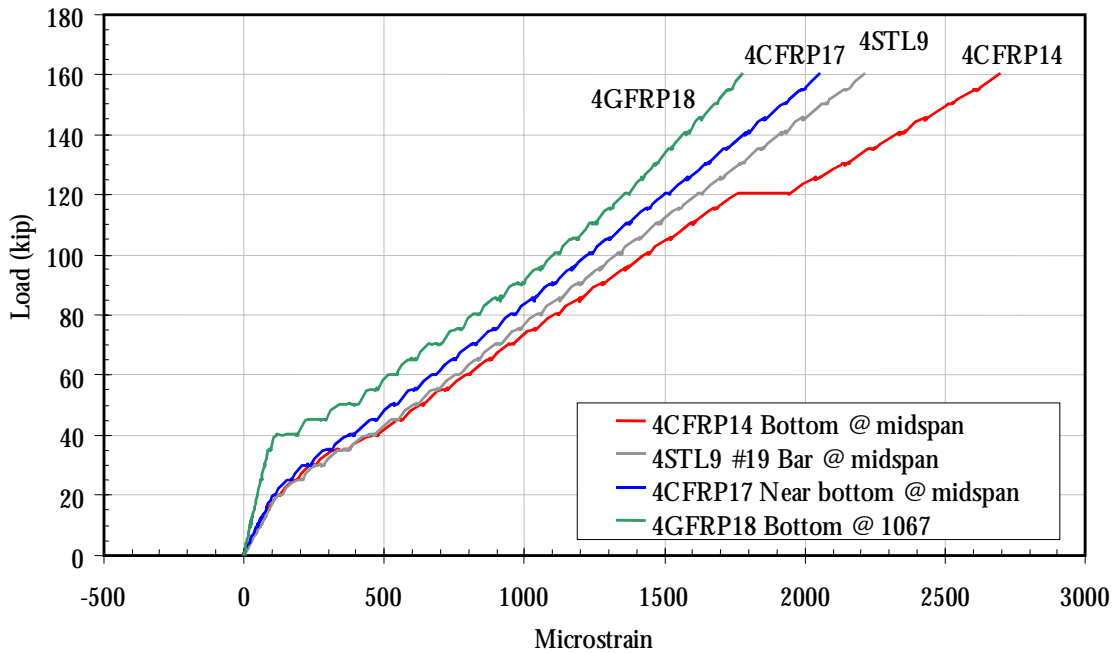


Figure C-27: S&F Beam tensile strain comparison

Table C-1: Resistance strain gauge identification

Gauge I.D. ¹	Coordinate Location ²			Gauge Description / Notes
	X (mm)	Y (mm)	Z (mm)	
1STL1	1067	106	667	Bent #19 rebar on C-D face of beam at the 1067 mm section and located in a horizontal orientation
1STL2	1067	127	508	Straight #16 rebar at the 1067 mm section
1STL3	1500	106	384	Bent #19 rebar on C-D face of beam at the 1500 mm section, located at 45 degree orientation and at midheight
1STL4	1500	127	508	Straight #16 rebar at the 1500 mm section
1CON5	1067	0	384	Midheight of 1067 mm section on the C-D face
1CON6	1500	0	384	Midheight of 1500 mm section on the C-D face
1STL7	1500	49	51	#22 rebar at the 1500 mm section closest to C-D face
1STL8	1067	49	51	#22 rebar at the 1067 mm section closest to C-D face
1CON9	1500	152	0	Beam bottom at the 1500 mm section
1CON10	1067	152	0	Beam bottom at the 1067 mm section
1STL11	3048	127	508	Straight #16 rebar at the midspan section
1CON13	3048	152	768	Beam top at the midspan section

Gauge I.D. ¹	Coordinate Location ²			Gauge Description / Notes
	X (mm)	Y (mm)	Z (mm)	
1CON14	3048	0	384	Midheight at the midspan section
1CON15	1500	152	768	Beam top at the 1500 mm section
1CON16	1067	152	768	Beam top at the 1067 mm section
1CON17	3048	152	0	Beam bottom at the midspan section
1STL18	3048	49	51	#22 rebar at the midspan section closest to C-D face
2CON1	1067	0	384	Beam midheight at the 1067 mm section
2FRP2	1067	152	-t _{FRP} ³	Beam bottom at the 1067 mm section
2FRP3	1500	152	-t _{FRP}	Beam bottom at the 1500 mm section
2STL5	1500	106	384	Bent #19 rebar on the A-D end at the midheight of the 1500 mm section (closest to C-D face, oriented at 45 degrees)
2STL7	3048	127	508	Straight #16 rebar at the midspan section
2FRP8	3048	-t _{FRP}	102-t _{FRP}	Side of beam at the midspan section located 102 mm from the bottom face of the CFRP surface
2STL9	4597	106	384	Bent #19 rebar at the midheight 4597mm from the B-C end (closes to C-D face, oriented at 45 degrees)
2FRP10	3048	152	-t _{FRP}	Beam bottom at the midspan section
2STL11	3048	152	51	#22 rebar at the midspan section (center bar of the three #22 rebars)
2CON12	3048	0	384	Beam midheight at the midspan section
2CON13	3048	152	768	Beam top at the midspan section
2SHRMID14				Middle gauge of 3 used for comparison to fiber optic shear gauges, see details
2SHRLOW15				Low gauge of 3 used for comparison to fiber optic shear gauges, see details
2SHRHIGH16				High gauge of 3 used for comparison to fiber optic shear gauges, see details
2CON17	1500	152	768	Beam top at the 1500 mm section
2CON18	1067	152	768	Beam top at the 1067 mm section
2CON19	1500	0	384	Beam midheight at the 1500 mm section
3CON1	1500	152	768	Beam top at the 1500 mm section
3CON2	1067	152	768	Beam top at the 1067 mm section
3STL3	1500	106	384	Bent #19 rebar on the A-D end at the midheight of the 1500 mm section (closest to C-D face, oriented at 45 degrees)
3FRP4	2134	-t _{FRP}	692	Located 76 mm from the top surface of beam under the load point on the C-D face and D end, located on the FRP surface and oriented horizontal

Gauge I.D. ¹	Coordinate Location ²			Gauge Description / Notes
	X (mm)	Y (mm)	Z (mm)	
3FRP5	2845	-t _{FRP}	692	Located 76 mm from the top surface of beam near midspan (203 mm from the midspan back toward A-D end, located on the FRP surface and oriented horizontal, located over an anchor
3FRP6	610	305+t _{FRP}	76-t _{FRP}	Vertically oriented gauge (only one this beam) located 610 mm from the A-D end of the beam on the A-B face and 76 mm from the beam bottom of GFRP
3STL7	3048	152	51	#22 rebar at the midspan section (center bar of the three #22 rebars)
3STL8	3048	106	51	Bent #19 rebar at the midspan section (closest to C-D face) oriented in a horizontal fashion
3FRP9	2845	235	-t _{FRP}	Beam bottom on FRP located 203 mm back from centerline toward A-D end and 70 mm from the A-B face
3CON10	3048	152	0	Beam bottom at the midspan section
3CON11	3048	0	384	Beam midheight at the midspan section
3STL12	3048	127	508	Straight #16 rebar at the midspan section
3CON13	3048	152	768	Beam top at the midspan section
3FRP14	1473	-t _{FRP}	384	Beam midheight at the 1500 mm section (25 mm toward the A-D end since the joint did not allow placement)
3FRP15	1067	-t _{FRP}	384	Beam midheight at the 1067 mm section
3FRP16	610	-t _{FRP}	76-t _{FRP}	Horizontally oriented gauge located 610 mm from the A-D end of the beam on the C-D face and 76 mm from the beam bottom of GFRP, opposite of gauge 6
3FRP17	1500	152	-t _{FRP}	Beam bottom at the 1500 mm section
3FRP18	1067	152	-t _{FRP}	Beam bottom at the 1067 mm section
3FRP19	305	-t _{FRP}	76-t _{FRP}	Located directly above the support on the A-D end on the C-D face, oriented horizontally 75 mm from the support face, similar to gauge 4
4FRP1	1500	-t _{FRP}	384	Beam midheight at the 1500 mm section (on a joint)
4FRP2	610	-t _{FRP}	76-t _{FRP}	Horizontally oriented gauge located 610 mm from the A-D end of the beam on the C-D face and 75 mm from the beam bottom of GFRP, opposite of gauge 6
4CON3	1500	152	768	Beam top at the 1500 mm section
4FRP4	1067	-t _{FRP}	384	Beam midheight at the 1067 mm section
4FRP5	610	305+t _{FRP}	3-t _{FRP}	Vertically oriented gauge (only for this beam) located 610 mm from the A-D end of the beam on the A-B face and 75 mm from the beam bottom of GFRP
4CON6	1067	152	768	Beam top at the 1067 mm section
4CON7	3048	152	768	Beam top at the midspan section

Gauge I.D. ¹	Coordinate Location ²			Gauge Description / Notes
	X (mm)	Y (mm)	Z (mm)	
4STL8	3048	127	508	Straight #16 rebar at the midspan section
4STL9	3048	199	51	Bent #19 rebar at the midspan section (closest to A-B face), oriented in a horizontal fashion
4STL10	3048	106	51	Bent #19 rebar at the midspan section (closest to C-D face), oriented in a horizontal fashion
4STL11	4597	106	384	Bent #19 rebar on the B-C end at the midheight of the 4597mm section (closest to C-D face, oriented at 45 degrees)
4CON12	3048	0	692	Beam midspan 75 mm from the top surface on the side of the beam
4CON13	3048	0	384	Beam midheight at the midspan section
4FRP14	3048	229	-t _{FRP}	Beam bottom at the midspan section (preferred gauge near the A-B face) located on the CFRP
4FRP15	3048	76	-t _{FRP}	Beam bottom at the midspan section (not preferred gauge near the C-D face) located on the CFRP
4FRP16	2134	-t _{FRP}	692	Located 75 mm from the top surface of beam under the load point on the C-D face and D end, located on the FRP surface and oriented horizontal
4FRP17	3048	-t _{FRP}	83	Beam midspan 686 mm from the top surface on the C-D side of the beam, located on the lapped up portion of CFRP
4FRP18	1067	241	-t _{FRP}	Beam bottom at the 1067 mm section (offset slightly to 89 mm from the A-B face)
4FRP19	1500	241	-t _{FRP}	Beam bottom at the 1500 mm section (offset slightly to 89 mm from the A-B face)

1. The first number in the gauge I.D. is the beam number (1=control, 2=Flexure-only, 3=Shear-only and 4 = Shear & Flexural FRP reinforced beam). The second part is the material that the gauge is applied to (e.g. STL = gauge on the steel reinforcing; CON=gauge applied to exterior concrete surface). The last number is the gauge number for that experimental beam.
2. Coordinates are measured from lower, right-hand corner in Figure C-28. X is distance along the beam span, Y is distance through the depth, and Z is the vertical distance.
3. The designation t_{FRP} is the thickness of the FRP reinforcement at that location. It is shown subtracted from or added to some coordinates to correctly fix the location of the gauges relative to the surface of the concrete. The thickness of the reinforcement varies with position on the beam.

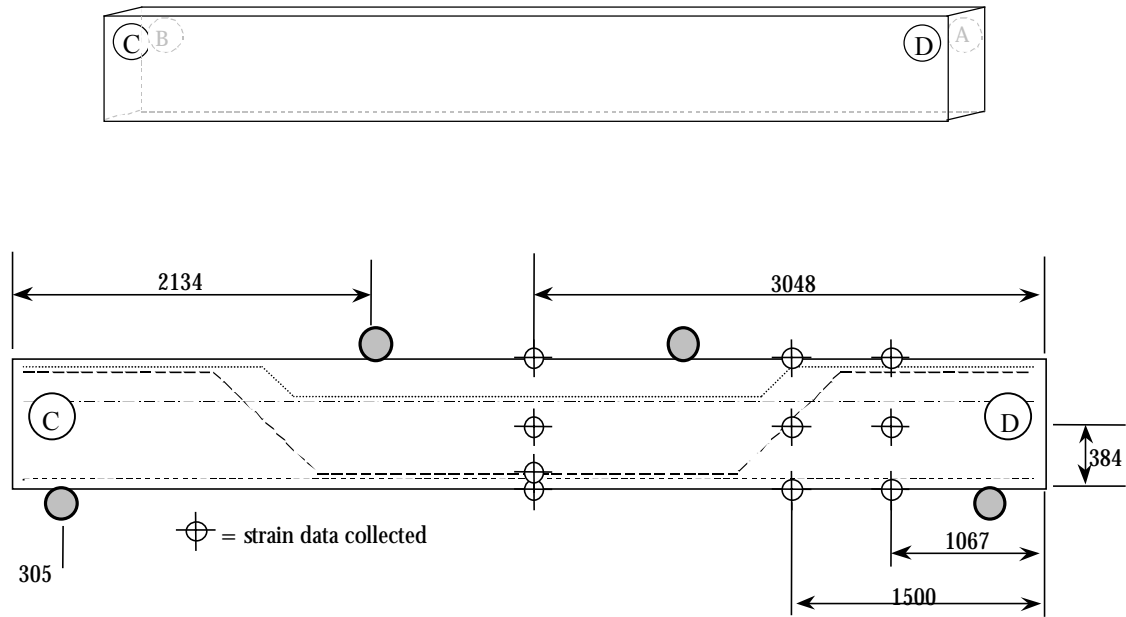


Figure C-28: Common resistance strain gauge locations (dimensions in mm)

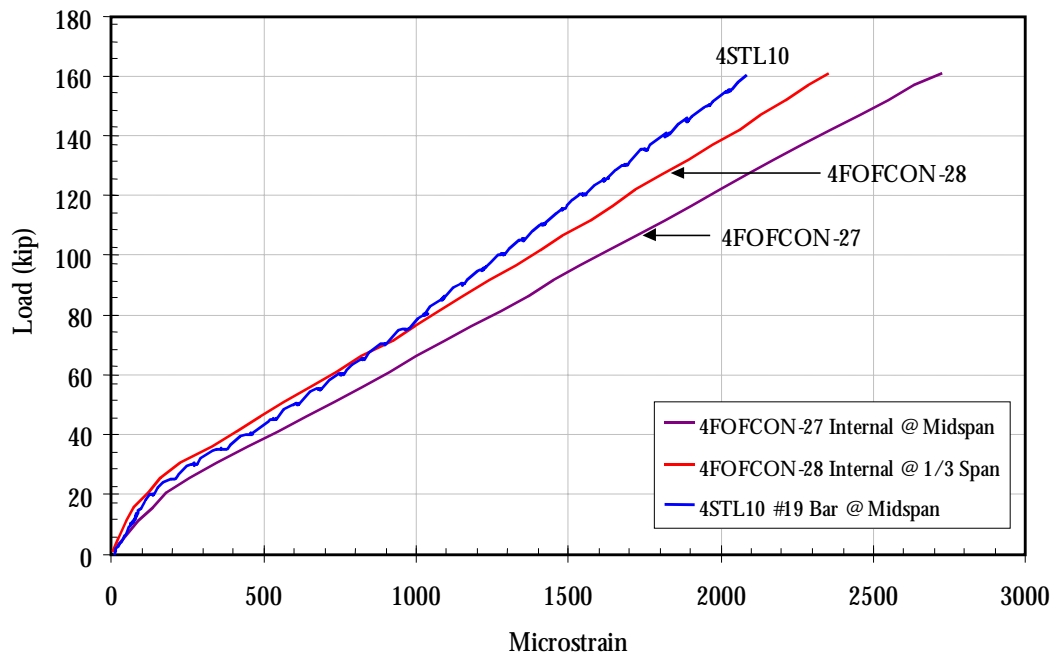


Figure C-29: Gauge type comparison—S&F Beam

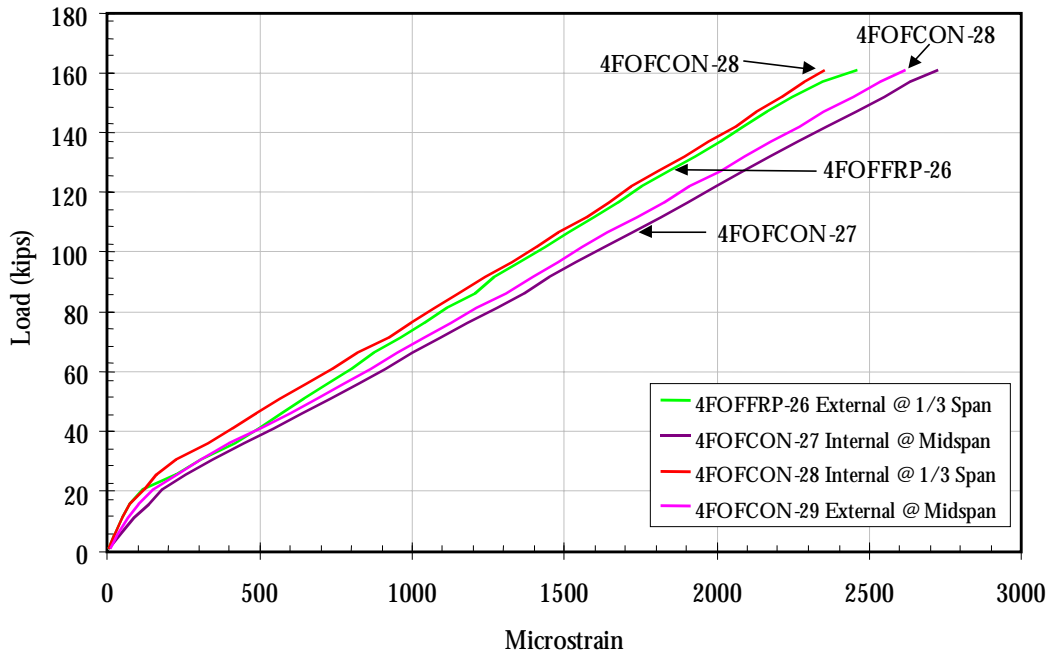


Figure C-30: Strain from flexural fiber optic strain gauges—S&F Beam

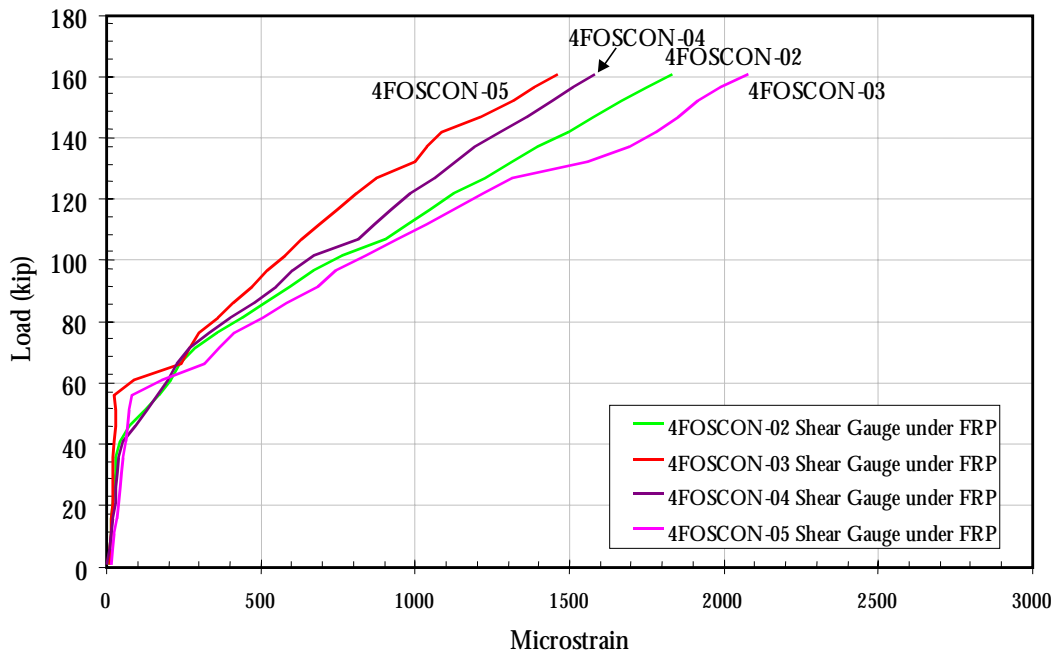


Figure C-31: Strain from shear fiber optic strain gauges embedded in concrete—S&F Beam

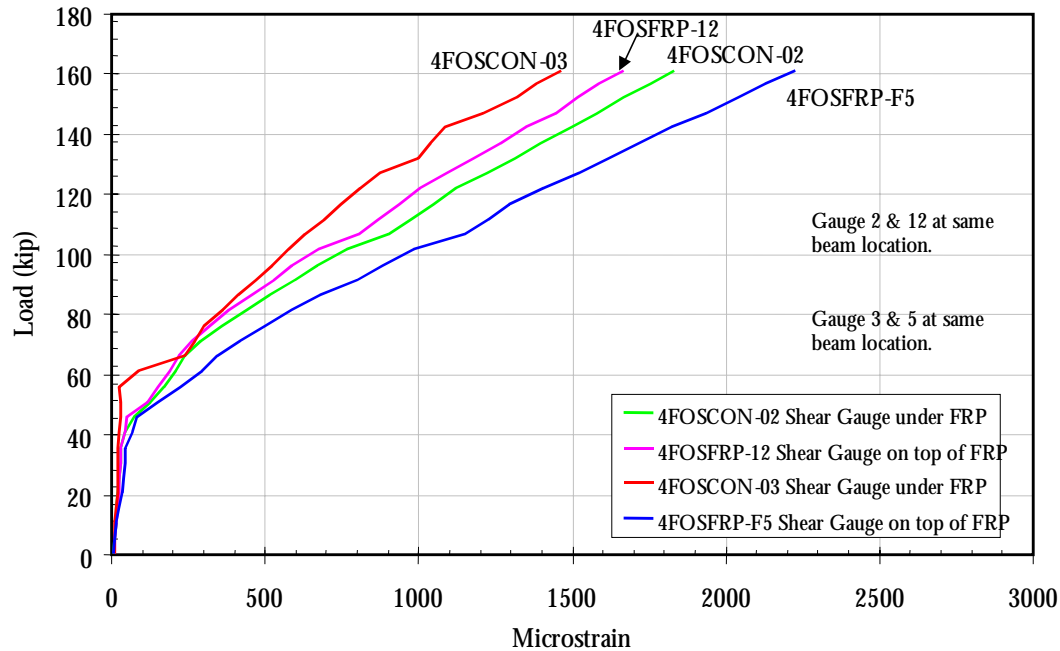


Figure C-32: Comparison of shear fiber optic strain gauges embedded in concrete and on top of the FRP reinforcement—S&F beam

Table C-2: Fiber optic strain gauge identification

Gauge I.D. ¹	Location ²			Gauge Description / Notes
	Gauge Length	Beam Side	Beam End	
4FOSCON-02	0.70 m	A-B	A-D	Shear gauge embedded in concrete
4FOSCON-03	0.70 m	C-D	B-C	Shear gauge embedded in concrete
4FOSCON-04	0.70 m	C-D	A-D	Shear gauge embedded in concrete
4FOSCON-05	0.70 m	A-B	B-C	Shear gauge embedded in concrete
4FOSFRP-F5	0.70 m	C-D	B-C	Shear gauge over FRP reinforcement
4FOSFRP-12	0.70 m	A-B	A-D	Shear gauge over FRP reinforcement
4FOFCON-24	1.00 m	Bottom	B-C	Flexure gauge embedded in concrete
4FOFFRP-26	1.00 m	Bottom	A-D	Flexure gauge over FRP reinforcement
4FOFCON-27	1.00 m	Bottom	Midspan	Flexure gauge embedded in concrete
4FOFCON-28	1.00 m	Bottom	Midspan	Flexure gauge over FRP reinforcement

1. The first number in the gauge I.D. is the beam number (4 = Shear & Flexural FRP reinforced beam). The first three letters are the strain intention (e.g. FOF = gauge intended to collect flexural strain at the beam bottom; FOS = gauge intended to collect strain in the high shear region). The second three letters are the material which the gauge is applied to (e.g. FRP = gauge on the exterior of the FRP composite; CON = gauge embedded in concrete surface, mostly under the FRP). The last number is the gauge number for that experimental beam.
2. See Figure C-33.

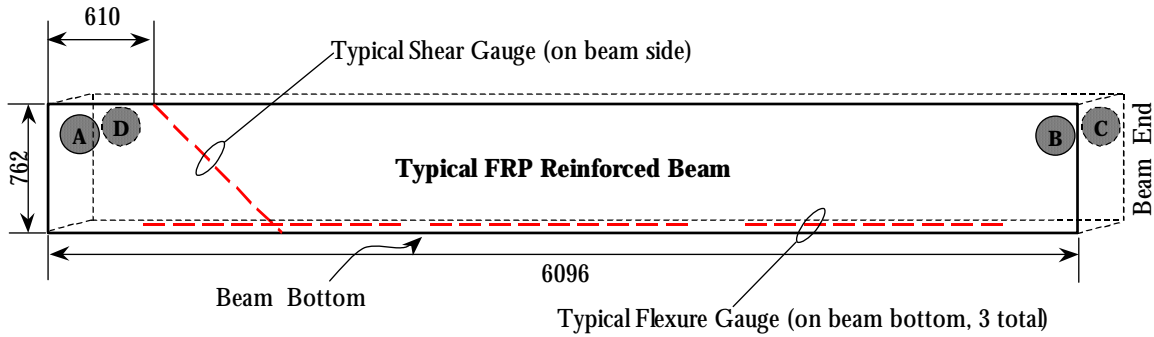


Figure C-33: Fiber optic strain gauge locations (dimensions in mm)

Crack Patterns

Flexural cracks are located near the midspan and are oriented nearly perpendicular to the long axis of the beam. Shear cracks are diagonal cracks that appear in the shear span (i.e. between the load and support points). A more appropriate term is diagonal tension cracks or inclined cracking. These cracks are the result of combined bending and shear forces realigning the principal tension direction (recall Mohr's circle of stress). The cracks only occur when bending forces are restrained and inclined cracking is unrestrained. A diagonal tension crack that propagates through the entire beam results in shear failure. Shear crack and diagonal tension crack are used interchangeably in the following discussion.

Cracking was thoroughly mapped in the Control and F-Only beams. The S-Only and S&F beam cracks were mostly concealed under the FRP reinforcement.

Control Beam Cracking

For this beam test, load was briefly held steady at selected load levels to document cracking. Cracking of the Control Beam followed expected behavior. Loading from zero to 15 kip (66.7 kN) did not produce any notable cracking. First cracks appeared around 18 kip (80 kN) near the midspan. These flexural cracks increased in length and quantity up to approximately 60 kips (267 kN) at which time the first evidence of shear cracks was visible. The critical shear cracks did not completely develop until near the ultimate load of 107 kip (476 kN). Critical shear cracks were fully visible on both ends of the beam. Ultimately, one crack propagated from the support to the load point at approximately a 45° angle resulting in failure. Figure C-34 shows cracking before ultimate load and the diagonal tension crack responsible for failure. Both high shear regions of the beam developed shear cracks, but the critical crack occurred on the A-D end of the Control beam.

Flexure-Only Beam Cracking

Flexure-Only Beam cracking patterns were similar to the Control Beam. This similarity was anticipated. As was observed with the Control Beam, a critical diagonal tension crack resulted in

beam collapse. This critical shear crack, shown in Fig. C-35, developed at a higher load (approx. 80 kip, 356 kN) than the Control Beam. A complete assessment of cracking is not possible since the CFRP covered the main portion of the beam where tension cracks developed. Visible cracks during the test were fewer in number and did not appear to propagate as high as the Control Beam test. The shear crack that developed in the F-only Beam was visibly wider than the crack in the Control Beam. This is likely due to the additional resistance provided by the CFRP allowing extended deflection beyond the formation of the diagonal tension crack. The failing crack formed on the B-C end of the beam.

Shear-only Beam Cracking

Very little evidence of cracking could be seen through the GFRP on the S-only beam. When cracking did affect the glass FRP composite, it was visible as a color change (whitening of the epoxy). This is shown in Fig. C-36. These tension cracks occurred just prior to ultimate load. Since the composite is unidirectional (vertical fibers only) these vertical cracks do little to reduce the vertical shear strength provided by the FRP (unless numerous cracks cause debonding). Ultimately, the concrete at the top-midspan crushed.

Shear & Flexure Beam Cracking

The only evidence of cracking on the fully strengthened beam was at the midspan. These tension cracks were slightly audible and visible at about 120 kip (534 kN). As the load approached the machine limit, these cracks only increased in length. Even during the second loading, cracking was only visible at the midspan section.

A comparison of the crack patterns is shown in Figure C-37. No effort was made to size the cracks for this study.



(a)



(b)

Figure C-34: Control Beam cracking (a) and crack responsible for failure (b)



Figure C-35: Diagonal tension crack responsible for failure of F-Only Beam



(a)



(b)

Figure C-36: S-Only Beam (a) and flexural cracks (darkened for contrast) in GFRP near ultimate load (b)

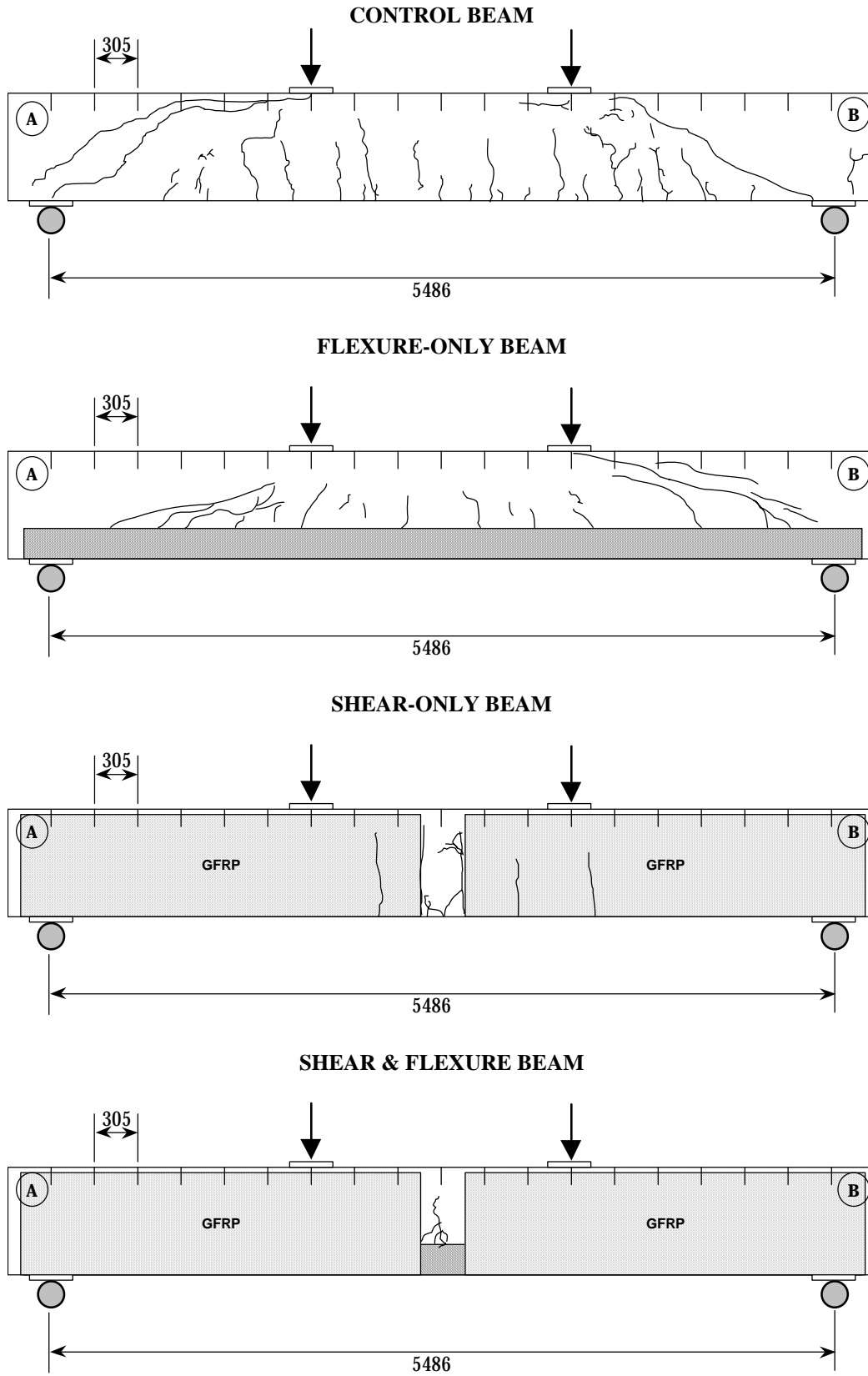


Figure C-37: Comparison of beam cracking (dimensions in mm)

Beam Failure Modes

Shear Failure of Control Beam

The Control Beam was deficient in shear as expected based on the load rating calculations shown in Appendix B. The Control Beam exhibited classical diagonal tension failure. It is possible that the designer/engineer of Horsetail Creek Bridge anticipated diagonal tension cracking, thus bending two of the five flexural bars through the high shear zone. It is more likely, however, that the bent steel was simply intended for negative moment reinforcement over the columns. The bent bars provided minimal reinforcement once the diagonal tension crack initiated.

Shear Failure of Flexure-Only Beam

The F-Only Beam failed in shear but at a higher load than the Control Beam. Since shear reinforcement was absent, the addition of CFRP for flexure was not expected to add shear strength. From a conventional design standpoint, horizontal structural components are not used to resist diagonal tension cracking. Diagonal tension cracks were visible at slightly elevated load levels over the Control Beam. However, since the CFRP was wrapped up the sides (see Figure 2-2), the CFRP was able to equilibrate forces across the diagonal tension cracks. In addition, the CFRP also increased the beams flexural rigidity reducing the strain for any given load in comparison to the Control Beam.

The CFRP fibers were able to maintain integrity of the beam in the presence of the shear crack. Since the fiber orientation was horizontal, the vertical strain component eventually reached a level that failed the matrix of the composite on the side of the beam. The shear cracks were then able to propagate completely through the beam.

It would be advantageous to apply a composite with strength in two principal directions to provide horizontal and vertical strength. The most effective resistance to diagonal tension cracks would be an FRP with its principal direction oriented orthogonal to the crack (aligned with the principal tension strains). The difficulty is predicting the beam response, since a composite with uniquely directional properties will be applied to a beam supposedly homogeneous and isotropic. To simplify the analysis considerably two separate systems might be applied to strengthen the beam. One system for flexure and one for shear (i.e. one horizontal and one vertical like the web and the flange in an I-beam). For construction simplicity, a single bi-directional system with orthogonal fibers could be used.

Flexural strengthening should not be used to increase the design shear capacity (although it was observed to). Predictability of this behavior is not reliable. If a moment deficiency exists, moment strengthening should be performed and vice versa for shear deficiency. For design, the F-Only Beam would have the same strength as the Control Beam and less than the S-Only Beam. Experimentally, it has an equivalent strength as the S-only beam. It was experimentally studied to examine the independent effect of flexural reinforcement with CFRP.

Flexural Failure of the Shear-Only Beam

The S-Only Beam showed the desired failure mode of a properly designed reinforced concrete beam. The GFRP reduced or eliminated the diagonal tension cracking and forced the beam into flexural failure at the midspan section. Figure 3-3 shows the main flexural steel yielded at approximately 120 kip (534 kN). The resulting reduction in flexural rigidity caused a rapid increase in deflection. Ultimately, the concrete crushed at the top midspan. A considerable amount of “ductility” was present in the S-Only Beam as indicated by the extended deflections occurring after the steel yielded. A good design must ensure that shear strength is always in excess of the flexural strength.

Failure of the Shear & Flexure Beam

The S&F Beam was loaded to and held at the capacity of the testing system, 160 kip (712kN). This loading configuration produced an applied moment of 480 kip-ft (651kN-m). A second loading was conducted with the load points closer together to produce an applied moment of 640 kip-ft (868 kN-m). Deflections were visible, but the beam did not exhibit signs of failure. The load was held for approximately 5 minutes with no indication of steel yielding, concrete crushing, or increased deflection.

Calculations indicate (see Appendix E) that the beam would be limited by crushing of the concrete. Concrete strains at the top-midspan location were approaching 0.0015 at the maximum applied load (refer to Figure C-26). Strains in the CFRP reinforcement at midspan were approaching 0.003 and strains in the main tension reinforcing steel were slightly in excess of 0.002. This is clear evidence to the projected failing sequence of the beam in which the steel yields, extended deflections result, the concrete crushes, and the FRP ruptures from substantial deflections.

Fiber Optic Strain Data

Much of the data collected from the fiber optic strain gauges were not useful for analyses required in this project. This was the result of two specific shortcomings: the 700mm and 1000mm gauge lengths were too long, and the +/-15 microstrain resolution of the instrumentation was not sensitive enough to discern lower strain levels.

One particular example of the gauge length problem is illustrated in Figures C-14, C-38, and C-39. A fiber optic sensor with a 27.6 in (700 mm) gauge length was situated in the shear zone. Three resistance gauges were positioned along the fiber optic sensor as shown. Analyses have shown that a strain gradient would exist at the end of the beam similar to the one shown in Figure C-39. Though the beam test had a shear crack and point loading, a strain gradient would have been present. Indeed, the strains shown in Figures C-14 and C-38 from the three resistance gauges qualitatively agree with Figure C-39. However, the results from the fiber optic strain sensor are an average over the long gauge length, which can not show the strain gradient.

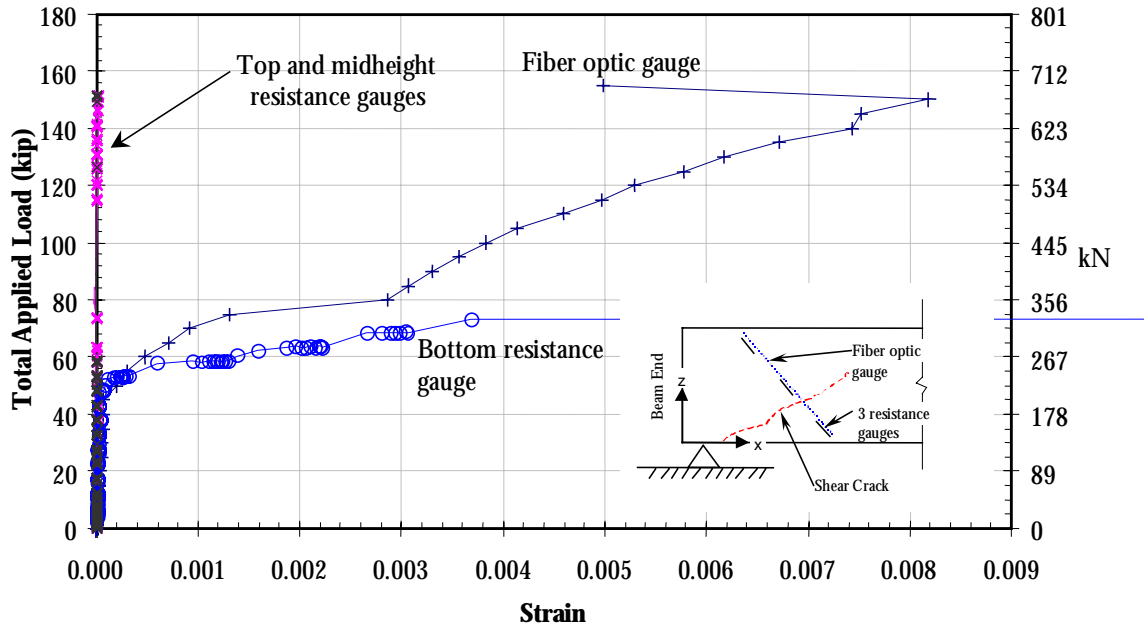


Figure C-38: Fiber optic vs. resistance strain gauge comparison—F-Only Beam

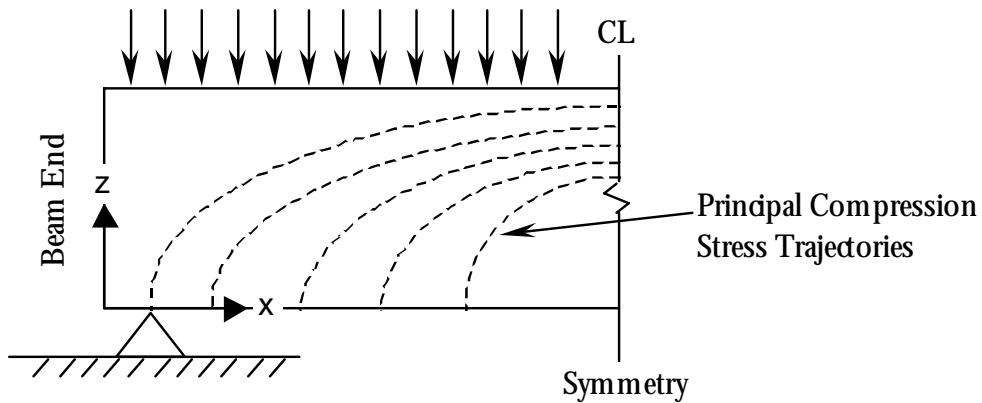


Figure C-39: Principal compression stress trajectories for a homogeneous simple beam uniformly loaded (after Nilson, 1997)

Fiber optic strain sensors are expected to play an important role in structural monitoring. For the strain sensors based on Bragg gratings (the type used in this project), the gauge length is easily varied from about 20mm to over 1500mm. In addition, recent advances in instrumentation have increased the sensitivity to less than one microstrain.

APPENDIX D: EQUIPMENT SPECIFICATIONS

APPENDIX D: EQUIPMENT SPECIFICATIONS

Sensor Equipment

Resistance Strain Gauges

Since strains were monitored on the internal steel reinforcement, on the concrete surface and on the surface of the FRP an appropriate gauge needed to be selected. To meet the needs of uniformity and economy, wire resistance gauges of 60-mm “active” length were chosen. These concrete-specific gauges were of sufficient length to integrate across aggregate non-uniformities on the beam surface. After adequate, but minimal preparation, these gauges were also easily applied to steel reinforcement (See Fig. A24, Appendix A).

Description: Wire resistance strain gauge with polyester backing; wire leads.

Manufacturer: Tokyo Sokki Kenkyujo Co., Ltd.

Distributor: (USA sales) Texas Measurements, Inc. 409-764-0442

Model: PL-60-11

Active Length: 60-mm

Resistance: 120-ohms

Gauge factor: 2.1

Displacement Transducers

Beam deflections were monitored at three points on the beam tension face (bottom). Linear Variable Differential Transformers (LVDT) powered with Direct-Current (DCDT) were chosen for ease of use and calibration. A style of DCDT with a loose core rather than a spring-loaded core was used to minimize the possibility of damage at beam failure.

Description: LVDT, DC powered (DCDT)

Manufacturer: Solartron Metrology

US offices: Buffalo NY 716-634-4452

Models used:

- ❖ DFG5 (serial no. 121316, nominal range +/- 5-mm)

Note: Type DFG5 = DCDT1

- ❖ DFG15 (serial no. 69784, nominal range +/- 15-mm)

Note: Type DFG15 = DCDT2

- ❖ DFG15 (serial no. 72870, nominal range +/- 15-mm)

Note: Type DFG15 = DCDT3

Mechanical Dial Indicator

Midspan deflections were measured using a dial indicator for all tests to confirm the results from DCDT measurements. Only one dial gauge was used, located at midspan (equivalent to DCDT2).

Description: Mechanical dial indicator

Range: 0-1 inch (small divisions 0.001 inch)

Manufacturer: Varies

Loading Machine

A 600-kip, hydraulic Baldwin Test Machine with a load-indicating dial equipped with a peak-indicating needle was used. In addition to the indicating needle, an electronic pressure sensor with signal conditioning provided a load signal. This load signal was monitored during all tests. The sensor was calibrated using the load dial as a standard. The load dial had been calibrated and certified within a year of all testing.

Fiber Optic Strain Sensing System

Strain Gauges

The fiber optic strain sensors were based on Bragg gratings. Nominal gauge lengths were 700mm and 1000mm.

Spectrum Analyzer

Ando Corporation AQ-6330 Optical Spectrum Analyzer. The window was set for 220 data points per nanometer (nm) so the smallest resolvable wavelength difference was approximately 5 picometers (pm). At a wavelength of 1300nm, 1pm was equivalent to 1 microstrain. The long-term resolution based on the manufacturer's specifications was +/-70 pm. Short term (within an hour) resolution was approximately +/-15 pm. The light sources used in conjunction with the spectrum analyzer were Optiphase, Inc. Broad Band Optical Source BBS-13-0150.

Demodulator

Blue Road Research Model BRR-3SA with a sensitivity of +/-150 microstrain over a dynamic range of +/-8000 microstrain. This demodulator had a built-in light source.

Data Acquisition

National Instruments, DAQCard-AI-16XE-50 with 16 analog inputs.

Pulse Velocity Tester

Manufacturer: CNS Farnell

Model: PUNDIT 6

Signal Conditioning and Data Acquisition Systems

Control Beam Test

Signal conditioning and data acquisition were achieved using a single hardware system manufactured by ADAC Corporation.

Signal Conditioning and Analog to Digital (A/D) Conversion

Description: Strain gauge bridge completion and preamplifiers were contained in a module with terminals for strain inputs, as well as for high-level signals. This module was connected via a 6-foot ribbon cable to a 12-bit A/D converter board, which resided in the Data Acquisition PC (personal computer).

Manufacturer: ADAC Corporation, Woburn, MA 01801, (781) 935-3200

Model No.: 4012BGEX (strain gauge amp and bridge completion); TB5525 & 5302EN (terminal board and enclosure) 5525MF (A/D board)

Personal Computer

486DX/66 IBM-compatible running Windows 3.11

Data Acquisition Software

LabTech Notebook for Windows, version 9.0 was used for data collection. This allowed real-time monitoring of signals and produced an ASCII record file in tabular form.

Flexure-Only Beam Test

Strain data from the Control Beam test was noisy. In addition, the ADAC strain measuring system was found to have insufficient strain zeroing capabilities. For these reasons, a more sophisticated strain measuring system by Hewlett Packard was obtained. This system was based on the HP 3852A scanning voltmeter, and HP Vee 5.0 software. The HP system had much wider zeroing capability, higher rejection of power-line-frequency noise and better strain resolution. For the Flexure-Only Beam test, the HP system was used to gather strains only; an entirely separate PC data system was used concurrently to log displacement and load data. A marker signal was applied, common to both systems, for synchronizing the systems. In addition, PC clocks were closely synchronized before testing.

A. Strain Monitoring

Signal Conditioning and A/D Conversion

Description: 5-½ -digit integrating voltmeter with terminal board, bridge completion and amplifiers for strain gauges.

Manufacturer: Hewlett-Packard Corp., Palo Alto CA 94303, (800) 452-4844

Model: 3852A mainframe with 44701A integrating voltmeter, 44705A relay multiplexer, and 44717A relay multiplexer for 120-ohm strain gauges.

Personal Computer

486DX/66 IBM-compatible; Windows 95

Data Acquisition Software

HP Vee for Win 95, version 5.0

B. Load and DCDT monitoring

Signal Conditioning and A/D Conversion

Description: PC data acquisition system with on-board signal conditioning and 14-bit A/D conversion.

Manufacturer: Validyne Engineering, Northridge, CA (800) 423-5851

Model: UPC-607

Personal Computer

486DX/66 IBM-compatible

Data Collection Software

Validyne “EasySense” for DOS

Shear-Only Beam Test

The HP 3852A/HP Vee system was further developed so load and displacements could be monitored along with all strains. A single PC and data system was used. All data were written to a single data file. Four to six strains of interest were plotted in real time for monitoring during the test.

Shear & Flexure Beam Test

This beam used the same system as the Shear-Only Beam test.

**APPENDIX E: DESIGN CALCULATIONS FOR FRP
RETROFITTED REINFORCED CONCRETE MEMBERS**

APPENDIX E: DESIGN CALCULATIONS FOR FRP RETROFITTED REINFORCED CONCRETE MEMBERS

The method used to design the FRP strengthening scheme for HCB is presented here as originally proposed (Kachlakev, 1998). The calculations are based on the actual materials used in the construction of the bridge and the experimental beams.

OSU Design Method

As suggested in Chapter 2, a design process for shear and flexure was used to predict the strength of the experimental beams, hereafter referred to as the OSU Method. The following assumptions are necessary for this design process to be valid.

Introduction and design philosophy

The adopted design philosophy is outlined below. FRP composite materials are considered brittle, because they exhibit linear stress-strain diagrams to failure. It should be noted that concrete is also considered a brittle material and yet, reinforced concrete flexural members exhibit ductile behavior at failure. In regular reinforced concrete design, this ductile behavior is achieved through limiting the amount of steel reinforcement in the balanced area, and assuring that steel yields prior to concrete crushing. Thus, the yielding of steel reinforcement converts the behavior of an otherwise brittle system to a ductile system. There is no reason to expect that the addition of another brittle material (FRP) to the already ductile system will result in a brittle failure, as long as the total area of the reinforcement is restricted to 75% or less of the balanced section.

It is known that the load-deflection curve of an under-reinforced beam consist of two regions, i.e., linear-elastic prior to steel yielding followed by ideally-plastic response afterward. Theoretically, this behavior is similar to the behavior exhibited by a FRP strengthened beam. With increasing cross sectional area of FRP reinforcement, the nearly horizontal ideally-plastic portion of the curve increases in slope, eventually becoming identical to that of the linear-elastic portion. At this point, the ductile behavior of the system (concrete-steel-FRP) changes to brittle behavior. When areas of FRP and steel reinforcement are in the prescribed limits, a significant change in the behavior of the system occurs at yielding of steel. Under very little increase of load, the deflections become excessive, thus allowing for redistribution of moments to areas of redundancy, and warning of impending failure.

The parameters that affect the strengthening design of reinforced concrete beams include the following factors: a) the effects of initial strain; b) FRP/steel reinforcement ratios; c) material properties of concrete, steel reinforcement and FRP composites; d) stress of the steel reinforcement at working loads; e) deflections under working loads, f) failure mechanisms, and g) behavior of the strengthened beam under service loads. The restrictions include considering flexural behavior only (shear is not considered) and assuming a pre-cracked concrete section.

General Assumptions

1. Classical beam theory assumptions apply.
2. Elastic and homogeneous concrete material.
3. Elastic-perfectly plastic steel reinforcement.
4. Linear elastic behavior of FRP materials up to failure.
5. Strength provided by components is the summation of parts (e.g. total shear strength is the strength of the concrete plus steel plus FRP).

Assumptions Specific to Flexure

- F1. Plane-cross sections remain plane during bending.
- F2. Five failure modes are possible.
- F3. Shear strength is in excess of flexural strength.

Assumptions Specific to Shear

- S1. Limiting FRP-concrete bond stress is 200 psi.
- S2. Limiting FRP-concrete interfacial strain is 0.004.

Flexural Design Input Requirements

The following two tables give the needed information to begin the strengthening design.

Table E-1: FRP strengthening input requirements for the actual bridge and experimental beams

Input	Variable	US Standard Value		Metric Value	
		Horsetail	Exper.	Horsetail	Exper.
Existing Concrete Section					
Area of tensile steel	$A_s =$	5.00 in ² $f_v = 33$ ksi	2.68 $f_v = 60$ ksi	3226 mm ²	1729
Area of compressive steel [‡]	$A_s' =$	0.00 in ²	0.00	0.0	0.0
Depth of tensile steel	$d =$	28.00 in	27.75	711 mm	705
Depth of compressive steel	$d' =$	0.0	0.0	0.0	0.0
Width of reinforced concrete section	$b =$	12.0 in	12.0	305 mm	305
Height of reinforced concrete section	$h =$	30.00 in	30.25	762 mm	768
Concrete clear cover cc	$cc =$	1.5 in	2.063	38 mm	52
cc + diameter/2	$c_s =$	2.0 in	2.50	51 mm	64
Beam Geometry					
Beam clear span length	$L_{cr} =$	240 in	216 in	6096 mm	5490

[‡] Small steel reinforcing bars do exist above the elastic neutral axis, but were found to be near the neutral axis after cracking and near ultimate and are disregarded for design. If compressive reinforcement is available and placed to increase the resisting C-force, it should be included in design.

Table E-2: Design material properties for the actual bridge beams and experimental beams

Input	Variable	US Standard Value		Metric Value	
		Horsetail	Exper.	Horsetail	Exper.
Concrete					
Compressive strength	$f_c' =$	2500 psi	3000	17.2 MPa	20.6
Elastic modulus [‡]	$E_c =$	2850 ksi	3120	19.7 GPa	21.6
Ultimate strain (crushing)	$\epsilon_{cu} =$	0.003	0.003	0.003	0.003
Steel Reinforcing					
Yield strength	$f_v =$	33 ksi	60	228 MPa	414
Elastic Modulus	$E_s =$	29,000 ksi	29,000	200 Gpa	200
Strain at yield	$\epsilon_v = f_v/E_s$.0011	.0021	0.0011	0.0021
CFRP Reinforcement [†]					
Reinforcement type	CARBON FABRIC (epoxy saturated, composite properties)				
Tensile strength	$f_{fu} =$	110 ksi		758 MPa	
Elastic modulus	$E_f =$	9,000 ksi		62.0 GPa	
Ultimate strain	$\epsilon_{fu} =$	0.0122		0.0122	
FRP thickness per ply	$t_f =$	0.041 in		1.04 mm	
GFRP Reinforcement [†]					
Reinforcement type	GLASS FABRIC (epoxy saturated, composite properties)				
Tensile strength	$f_{fu} =$	60 ksi		414 MPa	
Elastic modulus	$E_f =$	3,000 ksi		20.7 GPa	
Ultimate strain	$\epsilon_{fu} =$	0.02		0.02	
FRP thickness per ply	$t_f =$	0.051 in		1.30 mm	

[†] Design properties based on manufacturer literature. The same material was used for the experimental beams as was used to retrofit the actual bridge.

[‡] $E_c = 57000 (f_c')^{1/2}$

Loads and Existing Section Capacity

The information provided in this section is arranged to accommodate the load rating procedures as prescribed by ODOT and AASHTO (1989, 1994). In general, for flexural strengthening, a pre-retrofit moment capacity and required moment capacity will need to be provided. Accepted reinforced concrete theory should be used to calculate the existing section capacity.

Table E-3: Design loads and capacity input for actual bridge beams only

Input	Variable	US Standard Value	Metric Value
Live load moment	$M_{LL} =$	241 ft-kip [†]	326 kN-m
Dead load moment	$M_{DL} =$	107 ft-kip	145 kN-m
Total unfactored moment	$M_{WL} =$	355 ft-kip	481 kN-m
Existing section capacity	$M_{n,exist} =$	341 ft-kip	462 kN-m

[†] Not including impact factor.

Rating Factor

Conventional load rating requires the calculation of a rating factor. If the rating factor is below 1.0, the structural member is considered inadequate for the required load and accepted factors. Load rating of the HCB is presented in Appendix B. It was determined for flexure to be $RF = 0.50$, for HCB beams.

Design Procedure and Assumptions

Comments for the following calculations will be provided to clarify the procedure. A systematic process is given resulting in recommended FRP strengthening scheme.

Moment and Curvature at Steel Yield

Calculate the moment and curvature at yield for the unstrengthened section.

$$\rho_s = A_s / bd = (5.00 \text{ in}^2) / (12 \text{ in})(28 \text{ in}) = 0.0149 \quad [E-1]$$

$$n_s = E_s / E_c = (29,000 \text{ ksi}) / (2850 \text{ ksi}) = 10.18 \quad [E-2]$$

$$k = [(\rho_s * n_s)^2 + 2(\rho_s * n_s)]^{1/2} - (\rho_s * n_s) = 0.419 \quad [E-3]$$

$$c_y = (k)(d) = (0.419)(28.0 \text{ in}) = 11.74 \text{ in} \quad [E-4]$$

These commonly used equations assume elastic material behavior (particularly for the concrete). The equations are only valid for a singly reinforced concrete beam (i.e. neglecting the presence of any compression steel).

Concrete strain ϵ_{cy} at steel yield:

$$\epsilon_{cy} = \left(\frac{c_y}{d - c_y} \right) \left(\frac{f_y}{E_s} \right) = \left(\frac{11.74 \text{ in}}{28.00 \text{ in} - 11.74 \text{ in}} \right) \left(\frac{33 \text{ ksi}}{29,000 \text{ ksi}} \right) \quad [\text{E-5}]$$

$$\epsilon_{cy} = 0.00082 \text{ in/in}$$

Note that ϵ_{cy} is limited to $\frac{1}{2} \epsilon_{cu} = 0.003/2 = 0.0015$, in order to preserve the validity of the linear approximation.

Moment M_y at yielding of the steel reinforcement:

$$M_y = (A_s * f_y) (d - c_y / 3) \quad [\text{E-6}]$$

$$M_y = (5.00 \text{ in}^2 * 33 \text{ ksi}) (28.00 \text{ in} - 11.74 \text{ in} / 3) / 12$$

$$M_y = 331 \text{ ft-kip}$$

This equation is only valid for a singly reinforced section. The corresponding curvature at yielding of the steel reinforcement is calculated by

$$\phi_y = \epsilon_{cy} / c_y = (0.00082) / (11.74 \text{ in}) = 6.98 \times 10^{-5} \text{ in}^{-1} \quad [\text{E-7}]$$

Strain in the Beam at the Level of FRP Laminate

Assume that the dead load plus an additional 10% of the live load will be acting on the beam at the time of retrofit. Calculate the applied moment

$$M_{\text{retrofit}} = 0.1 * (248 \text{ ft-kip}) + (107 \text{ ft-kip}) = 132 \text{ ft-kip} \quad [\text{E-8}]$$

$$\phi_{\text{retrofit}} = (M_{\text{ret}} / M_y) (\phi_y) = (132 / 331) (6.98 \times 10^{-5} \text{ in}^{-1}) \quad [\text{E-9}]$$

$$\phi_{\text{retrofit}} = 2.79 \times 10^{-5} \text{ in}^{-1}$$

Assuming a linear slope of the moment curvature diagram.

Assume that the depth of the neutral axis equals that at yield when the beam is retrofit. This allows calculation of strain in the beam at the level of FRP laminate at the time of retrofit.

$$\epsilon_{b,\text{retrofit}} = (h - c_y) \phi_{\text{retrofit}} \quad [\text{E-10}]$$

$$\epsilon_{b,\text{retrofit}} = (30.0 \text{ in} - 11.74 \text{ in}) * 2.79 \times 10^{-5} \text{ in}^{-1} = 0.00051 \text{ in/in}$$

Area of the FRP Required to Resist the Ultimate Projected Moment

This calculation relies on the load rating procedure to find the required capacity.

$$RF_{\text{existing}} = \left[\frac{\phi M_n - \gamma_{DL} * M_{DL}}{DF * (1+I) \gamma_{LL} * M_{LL}} \right] \quad [E-11]$$

The rating factor for flexure was determine to be 0.5 for the existing HCB beams. Naturally, the FRP strengthened section should have a resistance factor of at least 1.0. The required moment capacity is then back calculated.

$$M_{\text{required}} = \frac{(RF = 1.0) * (1.033) * (1 + 0.10) * 1.3 * 241 + 1.2 * 107}{0.9} \quad [E-12]$$

$$M_{\text{required}} = 538 \text{ ft-kip}$$

The required resistance provided by the FRP is the current moment shortfall.

$$M_{\text{required}}^{\text{FRP}} = M_{\text{required}} - M_{\text{existing}} = 538 - 341 = 197 \text{ ft - kip} \quad [E-13]$$

Determination of the Failure Mode

To estimate the failure mode begin by calculating the depth of the neutral axis at the balanced condition.

$$c_{\text{bal}} = \frac{h * \epsilon_{cu}}{(\epsilon_{cu} + \epsilon_{fu} + \epsilon_{b,\text{retrofit}})} \quad [E-14]$$

$$c_{\text{bal}} = \frac{30.0 \text{ in} * 0.003}{(0.003 + 0.0122 + 0.00051)} = 5.72 \text{ in}$$

The use of the total section depth “h” as opposed to adding the distance to the centroid of the FRP composite is likely appropriate, since surface preparation will likely remove some material and the number of layers is yet unknown. Now, calculate the maximum area of tensile steel reinforcement to allow FRP rupture prior to concrete crushing.

$$A_{s,\text{max}} = \left[\frac{0.85 * f_c' * \beta * c_{\text{bal}} * b}{f_y} \right] \quad [E-15]$$

$$A_{s,\text{max}} = \left[\frac{0.85 * 2500 \text{ psi} * 0.85 * 5.72 \text{ in} * 12 \text{ in}}{33,000 \text{ psi}} \right] = 3.76 \text{ in}^2$$

$$A_{s,\text{max}} = 3.76 \text{ in}^2 < A_{s,\text{provided}} = 5.00 \text{ in}^2$$

This shows that crushing of the concrete will preclude rupture of the FRP laminate. Regardless of the selected FRP reinforcing, crushing of the concrete will control. This behavior will be common and depends largely on the geometry of the section.

Required FRP Area

For internal couple equilibrium, where $C = T$,

$$A_s * f_y + A_f * [(h-c)/c] * (0.003) - \epsilon_{b,retrofit} * E_f = (0.85) * f'_c * b * \beta * c \quad [E-16]$$

$$5 * 33,000 + A_f * [(30-c)/c] * (0.003) - 0.00051 * (9,000,000) = 0.85 * (2500) * 12 * (0.85) * c$$

$$A_f = (c^2 - 7.6125 * c) / (37.37 - 1.457 * c) \quad [E-17]$$

Equation for nominal moment capacity:

$$M_n = A_s * f_y * (d - \beta * c / 2) + A_f * f_f * (h - \beta * c / 2) \quad [E-18]$$

$$M_n = 5.0 * 33,000 * (28.0 - 0.85 * c / 2) + A_f * [(30 - c) / c] * (0.003) - 0.00051 * (9,000) * (30.0 - 0.85 * c / 2) = 6,456,000 \text{ in} \cdot \text{lb}$$

$$A_f = (26.1768 * c + c^2) / (346.509 - 18.4227 * c + 0.1914 * c^2) \quad [E-19]$$

Solving equations [E-17] and [E-19] simultaneously eliminates the unknown area of FRP.

Determine the neutral axis by reduction of the above. This results in,

$$c = 12.7331 \text{ in}$$

The required area of FRP reinforcing is then back calculated (equation [E-17] or [E-19])

$$A_{f,required} = 3.4647 \text{ in}^2$$

The required width of FRP reinforcement is,

$$b_{frp} = \frac{A_{f,required}}{t_f} = \frac{3.4647 \text{ in}^2}{0.041 \text{ in}^2 / \text{ply} - \text{in}} = 84.5 \text{ in} \quad [E-20]$$

Since most FRP materials are manufactured to specific widths and thickness, select the most appropriate configuration. In this case, 24 inch widths are available and providing 4 layers at 12 inches wide will be adequate. Thus,

$$A_{f,provided} = \frac{t_f}{b_{f,total}} = 4 * 0.041 \text{ in}^2 / \text{ply} - \text{in} * 24 \text{ in} = 3.936 \text{ in}^2 \quad [E-21]$$

Using the selected FRP area, determine the position of the neutral axis at ultimate load.

$$A_s * f_y + A_f * [((h - c_{ult}) / c_{ult}) * (0.003) - \epsilon_{b,retrofit}] * E_f = (0.85) * f_c' * b * \beta * c_{ult}$$

$$A_f = (c_{ult}^2 - 7.6125 * c_{ult}) / (37.37 - 1.457 * c_{ult})$$

$$c_{ult} = 13.10 \text{ in}$$

Note that, for this method, adding more area of FRP reinforcing will result in a predicted lowering of the neutral axis (c increases). Check the failure mode by,

$$\epsilon_{c,ult} = \left[\frac{c_{ult}}{h - c_{ult}} \right] * (\epsilon_{fu} + \epsilon_{b,ret}) \quad [E-22]$$

$$\epsilon_{c,ult} = 0.00969 \gg 0.003$$

which implies that crushing of the concrete controls.

The moment capacity after strengthening with FRP, according to equation [E-18] is,

$$M_n = 6,825,804 \text{ in-lb} = 569 \text{ ft-kip}$$

Following load rating requirements, the rating factor after strengthening can be calculated from [E-11]

$$RF_{retrofit} = \left[\frac{0.85 * 569 \text{ ft} - \text{kip} - 1.2 * 107 \text{ ft} - \text{kip}}{5.0 * (1 + 0.10) * 1.3 * 45 \text{ ft} - \text{kip}} \right] = 1.11 > 1.0$$

The retrofitted beam then satisfies strength requirements.

System Ductility Requirements

Curvature

The curvature at ultimate load is,

$$\psi_{ult} = \frac{\epsilon_c}{c} = \frac{0.003}{13.1 \text{ in}} = 2.29 \times 10^{-4} \text{ in}^{-1} \quad [\text{E-23}]$$

Or, checking against the FRP strains,

$$\psi_{ult} = \frac{\epsilon_{fu} + \epsilon_{b,ret}}{h - c} = \frac{(0.0122 + 0.00051)}{(30.0 \text{ in} - 13.10 \text{ in})} = 7.52 \times 10^{-4} \text{ in}^{-1} \quad [\text{E-24}]$$

Since the curvature using the FRP strain is tighter than using concrete crushing, concrete crushing controls the failure. A comparison of the moment and curvature at yield to ultimate is necessary to evaluate the ductility of the system. Consider the ratio

$$M_n/M_y = 569/331 = 1.72 \quad [\text{E-25}]$$

$$\psi_{ult} / \psi_y = 2.29/0.698 = 3.28 \quad [\text{E-26}]$$

NOTE:

- ❖ IF $M_n/M_y \geq 1.3$, THEN ψ_{ult} / ψ_y must be greater than 2.5
- ❖ IF $M_n/M_y < 1.3$, THEN ψ_{ult} / ψ_y must be greater than 2.0

In this case, both curvature requirements are satisfied.

Ductility Indices

For conventional design requirements, the ductility index μ shall be greater than 2.0. When moment redistribution is relied upon, μ shall be greater than or equal to 4.0. If seismic resistance of the system is essential for the design, μ shall be greater than or equal to 3.0. The ductility index is defined by

$$\mu = \frac{1}{2} \left[\frac{E_{total}}{E_{elastic}} + 1 \right] = \left[M_y * \frac{(M_y \psi_{ult} + M_n \psi_{ult} - M_n \psi_y)}{2M_n^2 \psi_y} \right] + 0.5 \quad [\text{E-27}]$$

$$\mu = 5.2 > 2.0$$

Ductility for general design requirements are satisfied.

Service Level Deflections

Calculations of moment of inertia and hence deflections will be consistent with current methods. That is, the FRP will be considered in the same manner as steel, transforming the respective area using a modular ratio. These calculations must be performed, but are omitted here, since they do not provide new insight into FRP strengthening.

Stresses and Strains Developed Under Working Loads

It is necessary to check service level stresses and compare against allowable values. These calculations are only necessary if the working load moment is greater than 80% of the yield moment. From before,

$$M_{WL}=355 \text{ k-ft} > 0.8 * M_y = 265 \text{ ft-kip} \quad [E-28]$$

The following conditions must be satisfied:

- ❖ Tensile Steel Reinforcing – $\epsilon_s \leq 0.80 * \epsilon_y$
- ❖ Concrete in Compression -- $\sigma_c \leq 0.45 * f_c'$
- ❖ FRP composite – $\epsilon_f \leq 0.30 * \epsilon_{fu}$

If these limits are not satisfied then serviceability will govern the design and the previously calculated reinforcing will need to be changed.

Elastic Stresses and Strains

For these calculations, assume that the provided FRP area will be used in design ($A_f = 3.936 \text{ in}^2$). Internal equilibrium is described by

$$C=T \quad [E-29]$$

Or,

$$0.5 * c * b * \epsilon_c * E_{c,eff} = A_s * E_s * \epsilon_s + A_f * E_f * \epsilon_f \quad [E-30]$$

The strain in the FRP is geometrically related by,

$$\epsilon_f = \left(\frac{h-c}{d-c} \right) \epsilon_s - \epsilon_{f,retrofit} \quad [E-31]$$

In addition, the concrete strain is related by,

$$\epsilon_c = \left(\frac{c}{d-c} \right) \epsilon_s \quad [E-32]$$

Since linear elastic behavior of the concrete is desired, the limiting strain of 0.002 in the concrete will be required. The effective elastic modulus is then,

$$E_{\text{eff}} = f_c' / 0.002 = 2500 \text{ psi} / 0.002 = 1.25 \times 10^6 \text{ psi} \quad [\text{E-33}]$$

The strain in the steel as related to the depth to the neutral axis is,

$$\epsilon_s = \frac{\epsilon_{b,\text{retrofit}}}{\left\{ \left[\frac{(h - c^2 * b * E_{\text{eff}})}{(d - c)} \right] + \frac{A_s * E_s}{A_f * E_f} \right\}} \quad [\text{E-34}]$$

$$\epsilon_s = \frac{0.00051}{\left\{ \left[\frac{(30.0 - c^2 * 12.0 * 1.25 \times 10^6)}{(28 - c)} \right] + \frac{5.0 * 29.0 \times 10^6}{0.984 * 9.0 \times 10^6} \right\}}$$

When simplified, equation [E-34] will give a quadratic relationship in the neutral axis location c . In order to develop another equation to solve simultaneously with [E-34], equate the applied moment to the resisting couple created by the tension reinforcement,

$$M_{\text{WL}} = A_s * E_s * \epsilon_s (d - c / 3) + A_f * E_f * \epsilon_f (h - c / 3) \quad [\text{E-35}]$$

Where

$$\epsilon_f = \epsilon_s \left[\frac{h - c}{d - c} \right] - \epsilon_{f,\text{ret}} \quad [\text{E-36}]$$

Combining equations [E-34] and [E-35] a solution for c should be achievable.

END OF FLEXURAL DESIGN

Shear Design Process

Designing an FRP reinforced beam for shear is different than flexure in that the strains of the FRP will be limited. Ultimate capacity (failure) calculations are not appropriate in this case, since strain limits the effectiveness of the concrete-FRP bond. For this reason, experimental studies have suggested that the strain in the FRP jacket be limited to a value of 0.004. Shear design is outlined as follows for the HCB beams and summarized for the experimental beams. For shear design, the use of the subscript “j” will designate the various properties of the FRP jacket. This notation will be useful in separating flexure and shear variables.

Concrete Shear Capacity

Typical reinforced concrete design will be used to calculate the concrete contribution to shear capacity. The shear capacity calculation here include the $d = 28''$ assumption. The actual bridge has a changing depth due to the roadway crowning. The calculations here are for comparison to experimental. The simplified capacity,

$$V_c = 2.0\sqrt{f'_c}(b)(d) \quad [E-37]$$

$$V_c = 2.0\sqrt{2500}(12)(28.0) = 33,600 \text{ lb} = 33.6 \text{ kips}$$

Steel Shear Capacity

In the case of the Horsetail Creek Bridge and the experimental beams, no stirrups were provided. Thus,

$$V_s = \frac{A_v f_y d}{s} = 0 \quad [E-38]$$

Shear Deficiency

Assuming that the total capacity is the sum of the constituent capacities, the required resistance of the FRP shear jacket is,

$$\phi V_j = V_{\text{demand}} - \phi[V_s + V_c] \quad [E-39]$$

$$\phi V_j = (89.2 \text{ kip} - 0.85(33.6 \text{ kip})) = 60.6 \text{ kip}$$

The FRP jacket must then resist a total force of 71.3 kips if a Φ -factor of 0.85 is used. This is the resistance to be provided by the FRP at a limited strain of 0.005.

Require FRP Jacket Thickness

$$tj \geq \frac{\phi V_j}{2\varepsilon_j E_j D(\cot \theta)} \quad [E-40]$$

Where θ is the angle between the shear crack and the principal direction of the FRP jacket fibers (assumed unidirectional). Using the known values,

$$tj \geq \frac{\phi V_j}{2\varepsilon_j E_j D(\cot 45)} \quad \text{for } 45 \text{ shear crack} = \frac{71.3 \text{ kips}}{2(0.005)(3000 \text{ ksi})(12'')(1)} = 0.198 \text{ in}$$

Required Number of Layers

$$\# \text{ layers} = \frac{t_j}{t_j / \text{layer}} = \frac{0.198}{0.051} = 3.88 \approx 4 \text{ layers} \quad [\text{E-41}]$$

Check Concrete Bond Stress

The bond stress is empirically limited to 200 psi. Thus,

$$\sigma_b = \frac{E_j t_j \epsilon_j}{l_d} = \frac{(3000 \text{ksi})(4 * .051)(0.005)}{12 \text{ in}} = 200 \text{ psi} \quad [\text{E-42}]$$

For this case, the bond is at its limit for the 12 in development length. Since the composite had more than 12 inches to develop bond, this requirement is satisfied.

Clearly, this method of design is very conservative. The required limitations are still in debate amongst the various researchers in FRP strengthening. The suggested 0.004 strain and 200 psi are conservative and this project was not able to suggest different values.

END OF SHEAR DESIGN

References

American Association of State and Highway Transportation Officials (AASHTO), 1994 Manual for Condition Evaluation of Bridges.

American Association of State and Highway Transportation Officials (AASHTO), 1989. Guide Specifications for Strength Evaluation of Existing Steel and Concrete Bridges.

Kachlakev, D.I., 1998. "Strengthening of the Horsetail Creek Bridge using Composite GFRP and CFRP Laminates," Special report prepared for the Oregon Department of Transportation.

Nanni, A., F. Focacci and C.A. Cobb, 1998. "Proposed Procedure for the Design of RC Flexural Members Strengthened with FRP Sheets," *Second International Conference on Composites in Infrastructure*, Tucson.

Nilson, A.H., 1997. Design of Concrete Structures, 12th Edition, McGraw-Hill: New York.

Whitney, C.S., and E. Cohen, 1957. "Guide for Ultimate Strength Design of Reinforced Concrete," *Journal of the American Concrete Institute*, ACI, Title No. 53-25, June, 1957.

Notation

Table E-4: Appendix E notation

Variable	Description	US Standard Units [†]	Metric Units [†]
A_f	Area of FRP	in ²	mm ²
$A_{f,required}$	Required area of FRP to resist the load demand	in ²	mm ²
A_s	Area of steel	in ²	mm ²
$A_{s,max}$	Maximum area of steel such that concrete compression controls	in ²	mm ²
$A_{s,provided}$	Provided area of steel reinforcing	in ²	mm ²
A'_s	Area of compression steel reinforcing	in ²	mm ²
b	Compression block width	in	mm
$b_{f,total}$	Total width of FRP to be provided	in	mm
b_{frp}	Width of FRP reinforcement	in	mm
c	Depth to the neutral axis from the top compression fiber	in	mm
$c_{balanced}$	Depth to the neutral axis at a balanced failure condition	in	mm
cc	Clear cover from concrete surface to near edge of steel	in	mm
c_s	Distance from the beam bottom to centroid of the steel	in	mm
$c_{ultimate}$	Depth to the neutral axis from the beam top at ultimate load	in	mm
c_y	Depth to the neutral axis from the beam top at steel yielding	in	mm
d	Structural steel depth from the beam top to the reinforcement	in	mm
d'	Structural steel depth of the compression reinforcement	in	mm
d_c	Structural depth to steel centroid	in	mm
DF	Distribution factor account for lane distribution of live load	~	~
DL	Total unfactored dead load	varies	varies
E_c	Modulus of elasticity of the concrete	psi	MPa
$E_{c,effective}$	Straight-line approximation of concrete elastic modulus	psi	MPa
$E_{elastic}$	Elastic modulus	psi	MPa
E_f	Elastic modulus of the FRP reinforcement	ksi	Gpa
E_s	Elastic modulus of the steel reinforcement	ksi	Gpa
E_{total}	Total elastic modulus of the beam	psi	MPa
f'_c	28-day specified concrete strength	psi	MPa
f'_{cu}	Todeschini stress-strain parameter	psi	MPa
f_{fu}	Ultimate stress (strength) of the FRP reinforcement	ksi	Gpa
h	Total overall depth of the concrete beam	in	mm
I	Impact factor applied to live loads as specified by AASHTO	~	~
j	Internal moment arm parameter	~	~
k	Internal moment arm parameter	~	~
L_{clr}	Beam span to center line of supports	ft	m
l_d	Bond development length	in	mm
LL	Total unfactored applied live load	varies	varies
M_{DL}	Moment caused by the total unfactored dead loads	ft-kip	kN-m
$M^{FRP}_{required}$	Require moment resistance to be provided by the FRP	ft-kip	kN-m

Variable	Description	US Standard Units [†]	Metric Units [†]
M_{LL}	Moment caused by the total unfactored live loads	ft-kip	kN-m
$M_{n,existing}$	Existing section moment capacity, prior to strengthening	ft-kip	kN-m
$M_{required}$	Required moment capacity to resist the applied loads	ft-kip	kN-m
$M_{retrofit}$	Total unfactored moment applied at the time of retrofit	ft-kip	kN-m
M_{WL}	Working load moment (services level loads)	ft-kip	kN-m
M_y	Moment at which the primary tension steel reinforcing yields	ft-kip	kN-m
n_s	Ratio of steel elastic modulus over concrete elastic modulus	~	~
RF	Load rating factor as defined by AASHTO	~	~
$RF_{existing}$	Existing section rating factor	~	~
$RF_{retrofit}$	Rating factor after retrofit of the beam	~	~
R_n	Nominal resistance (any mode)	varies	varies
t_f	Thickness of the FRP reinforcement per layer	in	mm
t_j	Thickness of the FRP jacket for shear strengthening	in	mm
V_c	Shear strength of concrete section alone	kips	kN
V_{demand}	Factored applied loads shear force demand on the sections	kips	kN
β	Equivalent stress block parameter for location of C-force	~	~
ϵ_0	Todeschini stress-strain parameter	~	~
$\epsilon_{b,retrofit}$	Strain at the time of retrofit at the level of FRP to be added	~	~
ϵ_c	Strain in the concrete top compression fiber	~	~
$\epsilon_{c,ultimate}$	Strain in the concrete top compression fiber at ultimate load	~	~
ϵ_{cu}	Ultimate (crushing strain of the concrete), typically 0.003	~	~
ϵ_{cy}	Strain in the concrete top compression fiber at steel yielding	~	~
ϵ_{fu}	Ultimate (rupture) strain of the FRP reinforcement	~	~
ϵ_s	Strain in the steel reinforcing	~	~
ϵ_y	Yield strain of the steel reinforcing	~	~
ϕ	General strength reduction factor	~	~
γ_{DL}	Dead load factor	~	~
γ_{LL}	Live load factor	~	~
μ	Ductility index	~	~
ρ_s	Tension steel reinforcement ratio, typically $A_s/(bd)$	~	~
σ_b	Bond stress limitation at FRP-concrete interface	psi	MPa
σ_c	Stress in the concrete	psi	MPa
$\Psi_{retrofit}$	Curvature at the time of retrofit	in^{-1}	mm^{-1}
Ψ_{ult}	Curvature at ultimate load	in^{-1}	mm^{-1}
Ψ_y	Curvature at yielding of the primary steel tension reinforcement	in^{-1}	mm^{-1}

[†] Typical units given. The use of “~” implies variable has no units.